Electronic Supplementary Information

Metal-catalyzed valence isomerization of a methylene(thioxo)phosphorane to a thiaphosphirane

Shintaro Ishida,* Yusuke Yoshida and Takeaki Iwamoto*

Department of Chemistry, Graduate School of Science, Tohoku University, Aoba-ku, Sendai 980-8578, Japan.

E-mail: ishida@tohoku.ac.jp, takeaki.iwamoto@tohoku.ac.jp

Contents

1. Experimental Details

General Procedures

All reactions treating air and moisture-sensitive compounds were carried out under argon and nitrogen atmosphere using a high-vacuum line and standard Schlenk techniques, or a glove box as well as dry and oxygen-free solvents. The ^{1}H, $^{13}C\{^{1}H\}$, ^{19}F, $^{29}Si\{^{1}H\}$, and $^{31}P\{^{1}H\}$ NMR spectra were recorded on a Bruker Avance III 500 FT NMR spectrometer. The ^{1}H and ^{13}C NMR chemical shifts (in ppm) were referenced to residual ^{1}H and ^{13}C of the solvents; benzene-d_6 (^{1}H δ 7.16 and ^{13}C δ 128.0). The ^{19}F NMR chemical shifts were relative to C_6F_6 in ppm. The $^{29}Si\{^{1}H\}$ NMR chemical shifts in C_6D_6 were relative to Me_4Si. The ^{31}P NMR chemical shifts in C_6D_6 were relative to 85% aqueous H_3PO_4. Sampling of air-sensitive compounds was carried out using a VAC NEXUS 100027 type glove box. Mass spectra (EI) were recorded on a JEOL JMS-Q1050 spectrometer. High-resolution mass spectra (HRMS) were performed on a JEOL JMS-T100GCV spectrometer using a FD+(eiFi) method. Melting points (mp) were measured by an OptiMelt MPA100 automated melting point system. Elemental analyses were performed on a J-SCIENCE LAB JM-11 at Research and Analytical Center for Giant Molecules (Graduate School of Science, Tohoku University). Analytical thin-layer chromatography (TLC) was performed on an aluminum plate coated with silica gel (0.25 mm thickness) containing a fluorescent indicator (silica gel 60F254, Merck). Flash silica gel column chromatography was performed on silica gel 60N (spherical and neutral gel, 40–50 μm, Kanto).

Materials

Hexane, benzene, toluene and THF were dried by using a VAC solvent purifier 103991. Diethyl ether (Et_2O) was dried over $LiAlH_4$. Benzene-d_6 (C_6D_6) was dried over molecular sieves MS 4Å. Acetone was dried over molecular sieves 3Å. PCl_3 was dried with potassium carbonate. Lithium, S_8, triethylamine and copper(I) chloride were commercially available and used without further purification. 1,1-Bis(dimethylphenylsilyl)ethylene **S1**[S1] and $AuC_6F_5(tht)$[S2] were prepared according to the published procedure.

Synthesis of Chlorophosphine 1

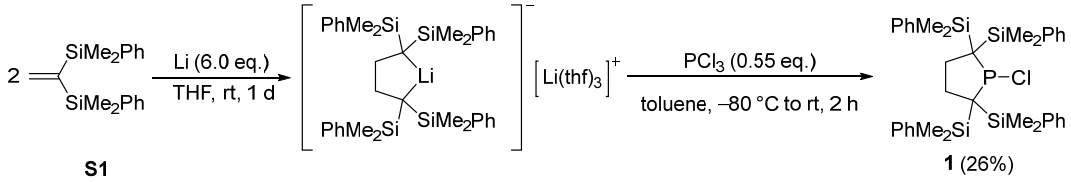

S1 **1** (26%)

In a Schlenk flask (100 mL) equipped with a magnetic stir bar, chopped lithium wires (0.76 g, 109 mmol), **S1** (5.43 g, 18.3 mmol) and THF (60 mL) were added, and the mixture was stirred for 1 day at room temperature. Then the resulting solution was transferred via a cannula to the other Schlenk flask (200 mL) equipped with a magnetic stir bar. After removal of THF in vacuo, dry benzene (70 mL) was added to the flask. To the solution, PCl_3 (1.38 g, 10.0 mmol) was added at −80 °C. The reaction mixture was allowed to warm gradually to room temperature over 2 hours. Insoluble materials were filtered off and the volatiles were removed from the filtrate in vacuo. Washing with acetone gave chlorophosphine **1** (1.59 g, 2.41 mmol) as colorless crystals in 26% yield.

1: colorless crystals; mp. 140-141 °C (decomp.); ^{1}H NMR (500 MHz, C_6D_6, 296 K, δ): 0.15 (d, 6H, $^{4}J_{PH}$ = 1.5 Hz, CH_3), 0.28 (d, 6H, $^{4}J_{PH}$ = 2.0 Hz, CH_3), 0.32 (s, 6H, CH_3), 0.36 (s, 6H, CH_3), 2.18-2.23 (m, 2H, CH_2), 2.73-2.79 (m, 2H, CH_2), 7.12-7.13 (m, 6H, Ph), 7.16-7.19 (m, 6H, Ph), 7.49-7.51 (m, 4H, Ph), 7.56-7.57 (m, 4H, Ph); ^{13}C{^{1}H} NMR (126 MHz, C_6D_6, 297 K, δ): 0.7 (d, CH_3, $^{3}J_{PC}$ = 11.0 Hz), 2.9 (s, CH_3), 3.1 (d, CH_3, $^{3}J_{PC}$ = 15.0 Hz), 4.1 (s, CH_3), 33.8 (d, C, $^{1}J_{PC}$ = 79.6 Hz), 36.9 (s, CH_2), 127.9 (s, CH), 128.0 (s, CH), 129.2 (s, CH), 129.6 (s, CH), 135.7 (d, CH, $^{4}J_{PC}$ = 3.5 Hz), 135.9 (s, CH), 139.9 (d, C, $^{3}J_{PC}$ = 4.4 Hz), 141.9 (s, C); ^{29}Si{^{1}H} NMR (99 MHz, C_6D_6, 296 K, δ): −1.3 (d, $SiMe_2Ph$, $^{2}J_{PSi}$ = 44.9 Hz), –0.3 (s, $SiMe_2Ph$); ^{31}P{^{1}H} NMR (202 MHz, C_6D_6, 296 K, δ) 199.4; MS (EI, 70 eV) *m*/*z* (%): 658 (1, M^+), 488 (19, $[M - Me_2PhSiCl]^+$), 135 (100, $[Me_2SiPh]^+$); Anal. calcd for $C_{36}H_{48}ClPSi_4$: C, 65.56%; H, 7.34%. Found: C, 65.17%; H, 7.40%.

Synthesis of Chlorophosphine Sulfide 2

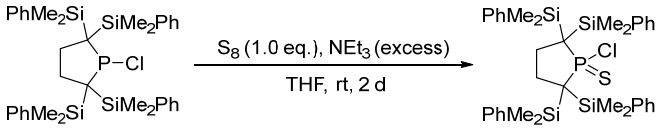

In a Schlenk flask (100 mL) equipped with a magnetic stir bar, **1** (670 mg, 1.02 mmol), S_8 (287 mg, 1.12 mmol), Et_3N (7 mL), and THF (28 mL) were added, and the mixture was stirred at room temperature for 2 days. After the removal of the volatiles, THF (50 mL) was added and the organic layer was washed with saturated Na_2SO_3 aqueous solution 9 times to remove the residual S_8, dried with $MgSO_4$ and the solvent was evaporated under reduced pressure. Washing the resulting yellowish brown solid with acetone and Et_2O provided chlorophosphine sulfide **2** as a white powder (460 mg, 6.67×10^{-1} mmol) in 65% yield.

2: a white powder; mp. 168-170 °C (decomp.); ^{1}H NMR (500 MHz, C_6D_6, 296 K, δ): 0.22 (s, 6H, CH_3), 0.44 (s, 6H, CH_3), 0.46 (s, 6H, CH_3), 0.51 (s, 6H, CH_3), 2.71-2.84 (m, 4H, CH_2), 7.05-7.08 (m, 6H, Ph), 7.10-7.13 (m, 6H, Ph), 7.37-7.39 (m, 4H, Ph), 7.58-7.59 (m, 4H, Ph); ^{13}C{^{1}H} NMR (126 MHz, C_6D_6, 296 K, δ): 2.2 (s, CH_3), 2.8 (s, CH_3), 3.2 (s, CH_3), 3.4 (s, CH_3), 34.8 (d, CH_2, $^{2}J_{PC}$ = 12.1 Hz), 43.8 (d, C, $^{1}J_{PC}$ = 13.1 Hz), 127.96 (s, CH), 127.97 (s, CH), 129.2 (s, CH), 129.4 (s, CH,), 136.1 (s, CH), 136.3 (s, CH), 141.0 (s, C), 141.0 (d, C, $^{3}J_{PC}$ = 11.3 Hz); ^{29}Si{^{1}H} NMR (99 MHz, C_6D_6, 297 K, δ): –0.55 (s, $SiMe_2Ph$), −0.51 (appeared as a shoulder peak at –0.55 ppm, $SiMe_2Ph$); ^{31}P{^{1}H} NMR (202 MHz, C_6D_6, 297 K, δ): 138.1; HRMS (FD+(eiFi)) (*m*/*z*): $[M]^+$ calcd for $C_{36}H_{48}ClPSSi_4$, 690.1980. Found: 690.1978; Anal. Calcd for $C_{36}H_{48}ClPSSi_4$: C, 62.52; H, 7.00%. Found: C, 62.46; H, 7.02%.

Synthesis of Methylene(thioxo)phosphorane 3

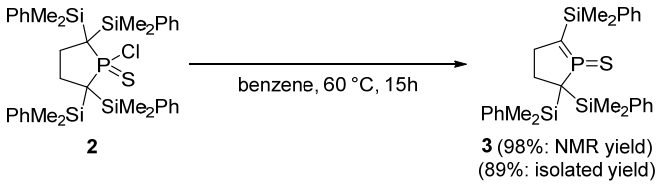

In a stock bottle (100 mL) equipped with a magnetic stir bar, **2** (950 mg, 1.44 mmol) and C_6H_6 (15 mL) were added, and then the mixture was stirred for 15 hours at 60 °C. Removal of benzene and chlorodimethylphenylsilane from

the reaction mixture in vacuo and subsequent recrystallization from hexane provided **3** (637 mg, 1.23 mmol) as colorless crystals in 89% yield. To estimate NMR yields, another experiment was carried out in a C_6D_6 (0.5 mL) solution using an NMR tube equipped with a J. Young valve. After the reaction, **3** and chlorodimethylphenylsilane formed in 98% and 100% yields, respectively, based on the ^{1}H NMR integrals using 1,3,5-tri(*tert*-butyl)benzene as an internal standard.

3: colorless crystals; mp. 75-78 °C; ^{1}H NMR (500 MHz, C_6D_6, 297 K, δ): 0.37 (s, 6H, CH_3), 0.45 (s, 6H, CH_3), 0.61 (s, 6H, CH_3), 1.58 (dt, 2H, CH_2, $^3J_{PH}$ = 34.5 Hz, $^3J_{HH}$ = 7.5 Hz), 2.09 (dt, 2H, CH_2, $^3J_{PH}$ = 16.5 Hz, $^3J_{HH}$ = 7.5 Hz), 7.14-7.21 (m, 9H, Ph), 7.33-7.34 (m, 2H, Ph), 7.64-7.66 (m, 4H, Ph); ^{13}C{^{1}H} NMR (126 MHz, C_6D_6, 298 K, δ): −1.9 (d, CH_3, $^3J_{PC}$ = 4.2 Hz), −1.8 (d, CH_3, $^3J_{PC}$ = 4.2 Hz), –0.9 (s, CH_3), 30.9 (d, CH_2, $^2J_{PC}$ = 15.9 Hz), 32.9 (d, CH_2, $^2J_{PC}$ = 16.4 Hz), 34.7 (s, C), 124.0 (d, C, $^1J_{PC}$ = 65.9 Hz), 128.0 (s, CH), 128.2 (s, CH), 129.3 (s, CH), 130.0 (s, CH,), 134.2 (s, CH), 135.3 (s, CH), 137.1 (d, C, $^3J_{PC}$ = 1.6 Hz), 138.8 (d, C, $^3J_{PC}$ = 7.4 Hz); ^{29}Si{^{1}H} NMR (99 MHz, C_6D_6, 296 K, δ): −11.3 (d, $SiMe_2Ph$, $^2J_{PSi}$ = 14.7 Hz), –1.1 (d, $SiMe_2Ph$, $^2J_{PSi}$ = 10.3 Hz); ^{31}P{^{1}H} NMR (202 MHz, C_6D_6, 297 K, δ): 211.9; HRMS (FD+(eiFi)) (*m*/*z*): $[M]^+$ calcd for $C_{28}H_{37}PSSi_3$: 520.1661. Found: 520.1661; Anal. calcd for C, 64.56; H, 7.16%. Found: C, 64.65; H, 7.19%.

Synthesis of Phosphaalkene 4

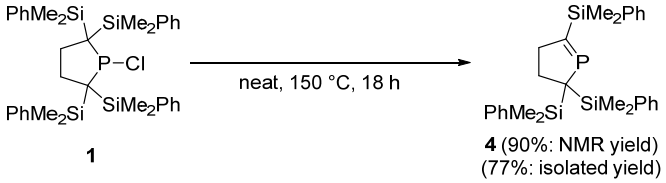

In a stock bottle (20 mL) equipped with a magnetic stir bar, **1** (201 mg, 3.05×10^{-1} mmol) was added and stirred for 18 hours at 150 °C. After the removal of chlorodimethylphenylsilane from the reaction mixture in vacuo, the obtained mixture was subjected to silica gel column chromatography (eluent: hexane; Rf = 0.1). Evaporation of the volatiles afforded **4** as a colorless viscous oil (114 mg, 2.33×10^{-1} mmol) in 77% yield. To estimate NMR yields, another experiment was carried out in a C_6D_6 (0.5 mL) solution using an NMR tube equipped with a J. Young valve. After the reaction, **4** formed in 90% yield based on the ^{1}H NMR integrals using 1,3,5-tri(*tert*-butyl)benzene as an internal standard.

4: a colorless viscous oil; ^{1}H NMR (500 MHz, C_6D_6, 296 K, δ): 0.26 (s, 6H, CH_3), 0.30 (s, 6H, CH_3), 0.45 (s, 6H, CH_3), 2.22-2.26 (m, 4H, CH_2), 7.14-7.24 (m, 9H, Ph), 7.42-7.43 (m, 2H, Ph), 7.53-7.54 (m, 4H, Ph); ^{13}C{^{1}H} NMR (126 MHz, C_6D_6, 298 K, δ): −1.67 (d, CH_3, $^3J_{PC}$ = 4.9 Hz), −1.5 (d, CH_3, $^3J_{PC}$ = 5.2 Hz), −1.4 (d, CH_3, $^3J_{PC}$ = 6.8 Hz), 35.0 (s, CH_2), 43.7 (d, C, $^1J_{PC}$ = 63.4 Hz), 45.4 (d, CH_2, $^2J_{PC}$ = 12.0 Hz), 127.9 (s, CH), 128.3 (s, CH), 129.3 (s, CH), 129.4 (s, CH), 134.2 (s, CH), 135.0 (s, CH), 138.9 (d, C, $^3J_{PC}$ = 4.8 Hz), 139.0 (s, C), 198.5 (d, P=*C*, $^1J_{PC}$ = 59.7 Hz); ^{29}Si{^{1}H} NMR (99 MHz, C_6D_6, 296 K, δ): −11.8 (d, $SiMe_2Ph$, $^2J_{PSi}$ = 32.1 Hz), –3.9 (s, $SiMe_2Ph$); ^{31}P{^{1}H} NMR (202 MHz, C_6D_6, 297 K, δ): 327.7; HRMS (FD+(eiFi)) (*m*/*z*): $[M]^+$ calcd for $C_{28}H_{37}PSi_3$: 488.1941. Found: 488.1940; Anal. calcd for C, 68.80; H, 7.63%. Found: C, 67.13; H, 7.68%. Although several attempts at careful elemental analysis have been made, the experimental data was not within ±0.4% of the theoretical value probably due to its high viscosity and instability in the air.

Isolation of Thiaphosphirane 5

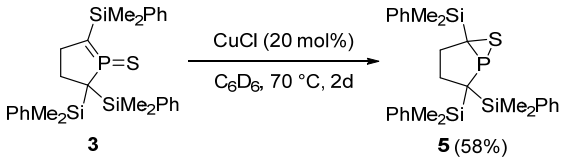

3 **5** (58%)

In a J. Young NMR tube, **3** (60 mg, 1.15 × 10^{-1} mmol), CuCl (2.4 mg, 2.42 × 10^{-2} mmol) and C_6D_6 (0.6 mL) were placed at 70 °C for 2 days. After filtration and evaporation of C_6D_6, the obtained mixture was subjected to silica gel column chromatography (eluent: hexane; Rf = 0.1). After the evaporation of the volatiles, **5** was obtained in 58% yield as an analytically pure colorless viscous oil (24 mg, 4.62 × 10^{-2} mmol). The oil was solidified as colorless crystals by recrystallization from a saturated hexane solution at room temperature.

5: colorless crystals; mp. 93-95 °C; ^{1}H NMR (500 MHz, C_6D_6, 295 K, δ): 0.10 (s, 3H, CH_3), 0.11 (s, 3H, CH_3), 0.30 (s, 3H, CH_3), 0.33 (s, 3H, CH_3), 0.36 (s, 3H, CH_3), 0.39 (s, 3H, CH_3), 1.77-1.90 (m, 2H, CH_2), 2.04-2.19 (m, 2H, CH_2), 7.13-7.23 (m, 9H, Ph), 7.40-7.42 (m, 2H, Ph), 7.45-7.47 (m, 2H, Ph), 7.62-7.64 (m, 2H, Ph); ^{13}C{^{1}H} NMR (126 MHz, C_6D_6, 300 K, δ): –3.2 (s, CH_3) –3.1 (d, CH_3, $^3J_{PC}$ = 5.5 Hz), –0.43 (d, CH_3, $^3J_{PC}$ = 10 Hz), –0.42 (s, CH_3), 0.1 (d, CH_3, $^3J_{PC}$ = 5.5 Hz), 0.2 (d, CH_3, $^3J_{PC}$ = 9.8 Hz), 25.4 (d, C, $^1J_{PC}$ = 72 Hz), 28.4 (s, CH_2), 35.7 (s, CH_2), 41.2 (d, C, $^1J_{PC}$ = 54 Hz), 127.9 (s, CH), 128.1 (s, CH), 128.2 (s, CH), 129.4 (s, CH), 129.65 (s, CH), 129.72 (s, CH), 134.7 (s, CH), 135.2 (s, CH), 135.4 (d, CH, $^4J_{PC}$ = 3.7 Hz), 138.1 (d, C, $^3J_{PC}$ = 1.3 Hz), 139.0 (d, C, $^3J_{PC}$ = 1.3 Hz), 139.4 (s, C); ^{29}Si NMR (99 MHz, C_6D_6, 299 K, δ): –2.4 (d, $SiMe_2Ph$, $^2J_{PC}$ = 14.9 Hz), -2.1 (d, $SiMe_2Ph$, $^2J_{PC}$ = 19.4 Hz), 1.3 (d, $SiMe_2Ph$, $^2J_{PC}$ = 1.9 Hz); ^{31}P{^{1}H} NMR (202 MHz, C_6D_6, 295 K, δ): –29.6; HRMS (FD+(eiFi)) (*m*/*z*): $[M]^+$ calcd for $C_{28}H_{37}PSSi_3$: 520.1661. Found: 520.1661; Anal. calcd for C, 64.56; H, 7.16%. Found: C, 64.60; H, 7.09%.

Synthesis of Thiaphosphirane Gold Complex 5Au

(a) From **3** in an NMR scale

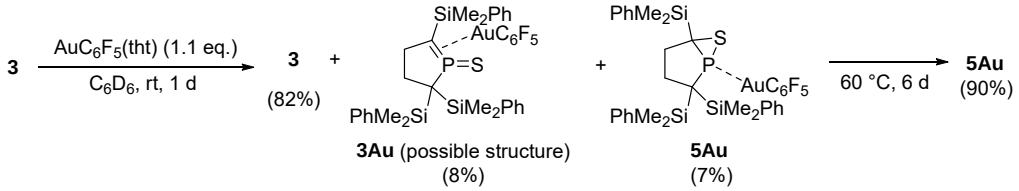

(b) From **5** in a preparative scale to isolate **5Au**

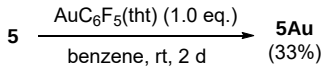

(a) From **3** in an NMR scale: In a J. Young NMR tube, **3** (10.2 mg, 1.96 × 10^{-2} mmol), AuC_6F_5(tht) (10 mg, 2.23 × 10^{-2} mmol) and C_6D_6 (0.5 mL) were placed at room temperature for 1 day. The NMR spectra (Figs. S40 and S41) indicated that a mixture of methylene(thioxo)phosphorane gold(I) complex **3Au** and thiaphosphirane gold(I) complex **5Au** were formed in 8% and 7% yield, respectively. Starting material **3** remained in 82%. Then, the reaction mixture was heated at 60 °C for 6 days. The NMR spectra indicated that **3** and **3Au** completely disappeared, and **5Au** formed

in 90% yield. The yields of the products were determined by ^{1}H NMR spectrum using 1,3,5-tri(*tert*-butyl)benzene as an internal standard.

(b) From **5** in a preparative scale to isolate **5Au**: In a stock bottle (20 mL) equipped with a magnetic stir bar, **5** (74 mg, 1.42×10^{-1} mmol), AuC_6F_5(tht) (71 mg, 1.57×10^{-1} mmol) and benzene (3 mL) were added and stirred for 1 day at room temperature in the dark. Then, the reaction mixture was filtered off and the filtrate was evaporated under reduced pressure. The obtained mixture was subjected to silica gel column chromatography (eluent: hexane; Rf = 0.1). Evaporation of the volatiles afforded **5Au** as a colorless solid (42 mg, 4.75×10^{-2} mmol) in 33% yield.

5Au: colorless solid; mp. 91-93 °C; ^{1}H NMR (500 MHz, C_6D_6, 295 K, δ): 0.19 (s, 3H, CH_3), 0.21 (s, 3H, CH_3), 0.36 (s, 3H, CH_3), 0.41 (s, 3H, CH_3), 0.43 (s, 3H, CH_3), 0.45 (s, 3H, CH_3), 1.66-1.80 (m, 3H, CH_2) 1.91-1.99 (m, 1H, CH_2), 7.13-7.20 (m, 9H, Ph), 7.40-7.42 (m, 2H, Ph), 7.48-7.50 (m, 2H, Ph), 7.54-7.55 (m, 2H, Ph); ^{13}C{^{1}H} NMR (126 MHz, C_6D_6, 296 K, δ): −3.4 (s, CH_3), −3.3 (s, CH_3), −0.15 (d, CH_3, $^3J_{PC}$ = 5.3 Hz), −0.09 (d, CH_3, $^3J_{PC}$ = 1.5 Hz) 0.0 (d, CH_3, $^3J_{PC}$ = 4.3 Hz), 1.1 (d, CH_3, $^3J_{PC}$ = 2.8 Hz), 29.4 (d, C, $^1J_{PC}$ = 31.1 Hz), 28.7 (s, CH_2), 34.2 (d, CH_2, $^2J_{PC}$ = 3.2 Hz), 38.6 (d, C, $^1J_{PC}$ = 17.1 Hz), 128.3 (s, CH), 128.5 (s, CH), 128.6 (s, CH), 130.3 (s, CH), 130.4 (s, CH), 130.5 (s, CH), 134.7 (s, CH), 135.3 (s, CH), 135.9 (s, CH), 136.0 (d, C, $^3J_{PC}$ = 3.0 Hz), 136.91 (s, C), 136.93 (s, C), 139.1 (m, C), 141.1 (m, C), 148.7 (m, C), 150.5 (m, C); ^{19}F NMR (470 MHz, C_6D_6, 295 K, δ): −161.9 to –161.7 (m), −157.5 (t, $^3J_{FF}$ = 20.2 Hz), −115.2 to –115.1 (m); ^{29}Si{^{1}H} NMR (99 MHz, C_6D_6, 295 K, δ): −2.3 (d, $SiMe_2Ph$, $^2J_{PSi}$ = 4.9 Hz), −0.8 (d, $SiMe_2Ph$, $^2J_{PSi}$ = 9.5 Hz), 1.6 (d, $SiMe_2Ph$, $^2J_{PSi}$ = 1.8 Hz); ^{31}P{^{1}H} NMR (202 MHz, C_6D_6, 296 K, δ): 32.0 (quint, $^4J_{FP}$ and $^5J_{FP}$ = 8.9 Hz); HRMS (FD+(eiFi)) (*m*/*z*): $[M]^+$ calcd for $C_{34}H_{37}AuF_5PSSi_3$: 884.1247. Found:884.1245; Anal. Calcd for C, 46.15; H, 4.21%. Found: C, 46.33; H, 4.41%.

Synthesis of Thiaphosphirane Sulfide 6

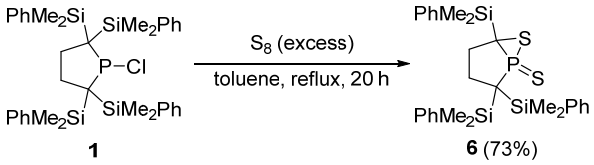

In a two necked flask (30 mL) equipped with a magnetic stir bar, chlorophosphine **1** (53 mg, 8.04×10^{-2} mmol), dry toluene (3 mL) and S_8 (190 mg, 0.741 mmol) were added, and the mixture was stirred for 20 hours under reflux condition. Then, the reaction mixture was filtered off and the filtrate was evaporated under reduced pressure. The obtained crude mixture was subjected to silica gel column chromatography (eluent: hexane; Rf = 0.05) to give **6** (32 mg, 5.84×10^{-2} mmol) as a white solid in 73% yield.

6: a white solid; mp. 101-103 °C; ^{1}H NMR (500 MHz, C_6D_6, 296 K, δ): 0.40 (s, 3H, CH_3), 0.41 (s, 3H, CH_3), 0.43 (s, 3H, CH_3), 0.47 (s, 3H, CH_3), 0.53 (s, 3H, CH_3), 0.59 (s, 3H, CH_3), 1.40-1.51 (m, 1H, CH_2) 1.80-1.92 (m, 3H, CH_2), 7.11-7.18 (m, 9H, Ph), 7.50-7.54 (m, 4H, Ph), 7.56-7.58 (m, 2H, Ph); ^{13}C{^{1}H} NMR (126 MHz, C_6D_6, 297 K, δ): −3.9 (s, CH_3), −3.4 (d, CH_3, $^3J_{PC}$ = 1.5 Hz), −0.9 (d, CH_3, $^3J_{PC}$ = 4.7 Hz), −0.5 (s, CH_3), 1.2 (d, CH_3, $^3J_{PC}$ = 2.5 Hz), 1.3 (s, CH_3), 29.3 (d, C, $^1J_{PC}$ = 9.2 Hz), 29.6 (d, CH_2, $^2J_{PC}$ = 4.3 Hz), 32.9 (d, CH_2, $^2J_{PC}$ = 10.8 Hz), 37.0 (d, C, $^1J_{PC}$ = 9.5 Hz), 128.0 (s, CH), 128.1 (s, CH), 128.3 (s, CH), 129.9 (s, CH), 130.0 (brs, CH, two signals were overlapped), 134.7 (s, CH), 135.5 (s, CH), 136.0 (s, CH), 137.0 (d, C, $^3J_{PC}$ = 4.5 Hz), 137.5 (d, C, $^3J_{PC}$ = 4.0 Hz),

138.0 (d, C, $^{3}J_{PC}$ = 4.5 Hz); $^{29}Si\{^{1}H\}$ NMR (99 MHz, C_6D_6, 296 K, δ): −2.2 (s, $SiMe_2Ph$), 0.2 (s, $SiMe_2Ph$), 1.4 (d, $SiMe_2Ph$, $^{2}J_{PSi}$ = 6.0 Hz); $^{31}P\{^{1}H\}$ NMR (202 MHz, C_6D_6, 297 K, δ): 42.0; MS (EI, 70 eV) *m*/*z* (%) 552 (11, $[M]^+$), 520 (2, $[M - S]^+$), 417 (3, $[M - SiMe_2Ph]^+$), 385 (8, $[M - S - SiMe_2Ph]^+$), 135 (100, $[Me_2SiPh]^+$); Anal. calcd for $C_{28}H_{37}PS_2Si_3$: C, 60.82; H, 6.74%. Found: C, 60.58; H, 6.74%.

Estimation of Thermodynamic Parameters

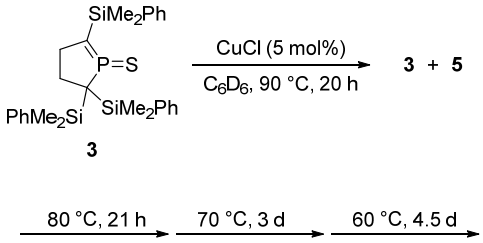

temperature	ratio **3** : **5**
90 °C	1 : 5.96
80 °C	1 : 6.60
70 °C	1 : 7.33
60 °C	1 : 8.17

In a J. Young NMR tube, **3** (106 mg, 2.04×10^{-1} mmol), CuCl (1.1 mg, 1.11×10^{-2} mmol) and C_6D_6 (0.6 mL) were placed at 90 °C for 20 h. The proceeding of the reaction was monitored by NMR spectroscopy. After the equilibrium has reached, the ratio of **3**:**5** was determined to be 1:5.96. Similarly, equilibrium constants at 80, 70, and 60 °C were estimated. A van't Hoff plot (ln*K* versus 1/*T* plot) is shown in Fig. S1, and the thermodynamic parameters were determined to be $\Delta H = -10.6 \pm 0.09$ kJ·mol^{-1}, $\Delta S = -14.2 \pm 0.26$ J·mol^{-1}·K^{-1}, and $\Delta G_{298} = -6.4$ kJ·mol^{-1}.

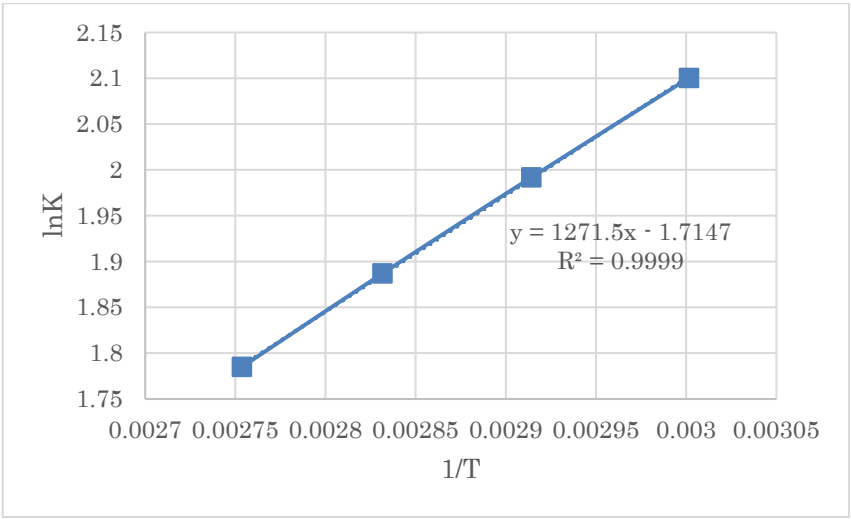

Fig. S1 A van't Hoff plot for the isomerization of **3** to **5**.

2. NMR Spectra

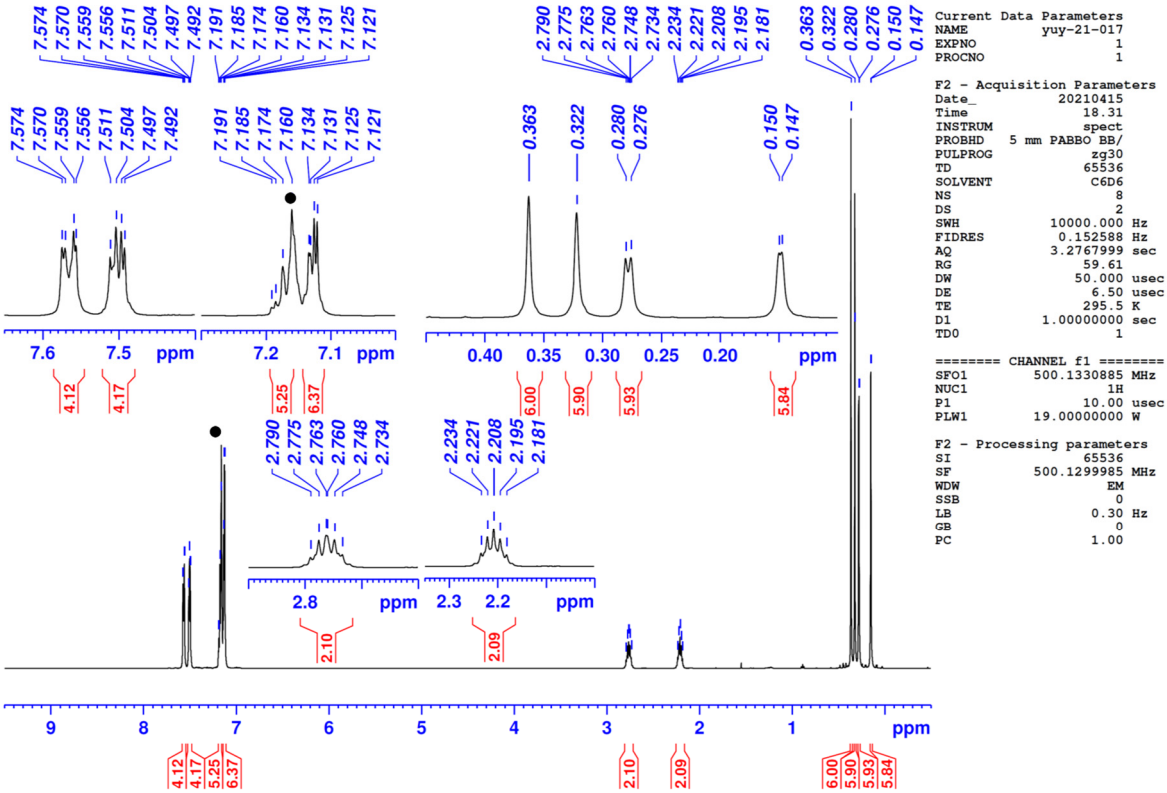

Fig. S2 ^{1}H NMR spectrum of **1** in C_6D_6 at 296 K (• = C_6HD_5).

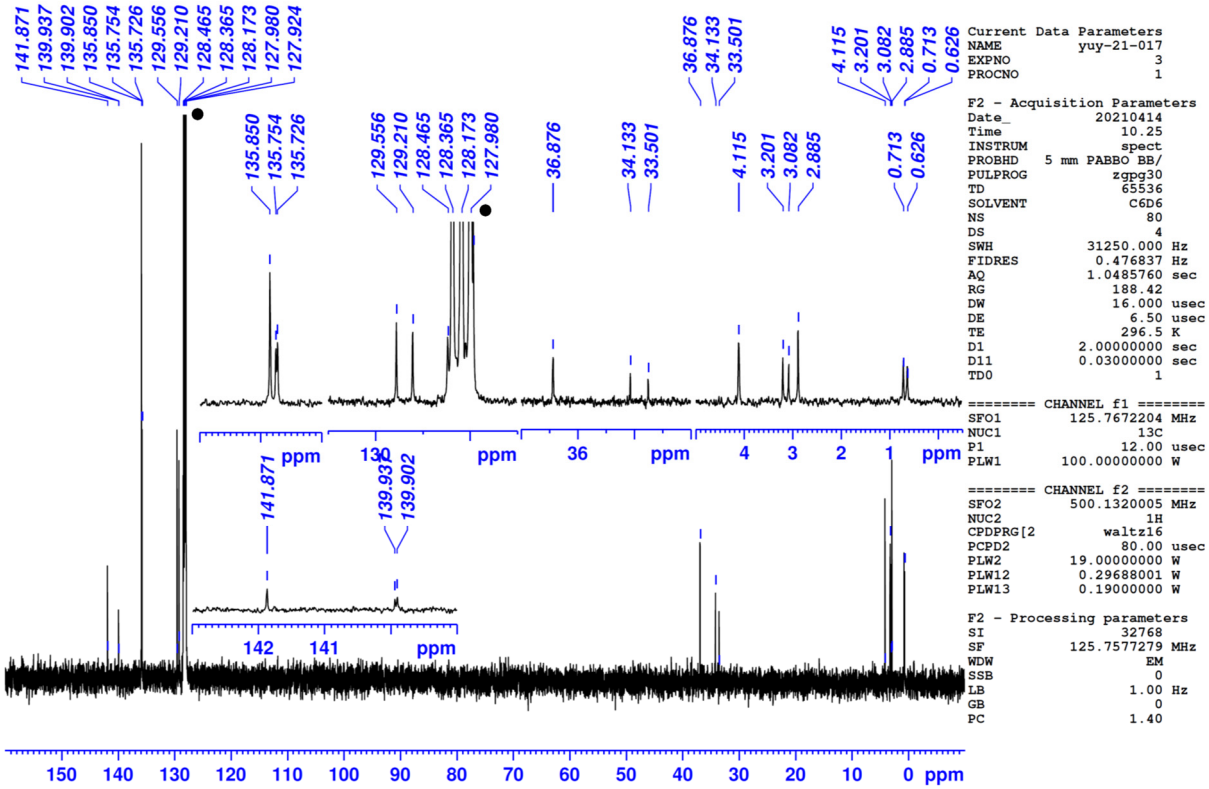

Fig. S3 ^{13}C{^{1}H} NMR spectrum of **1** in C_6D_6 at 297 K (• = C_6D_6).

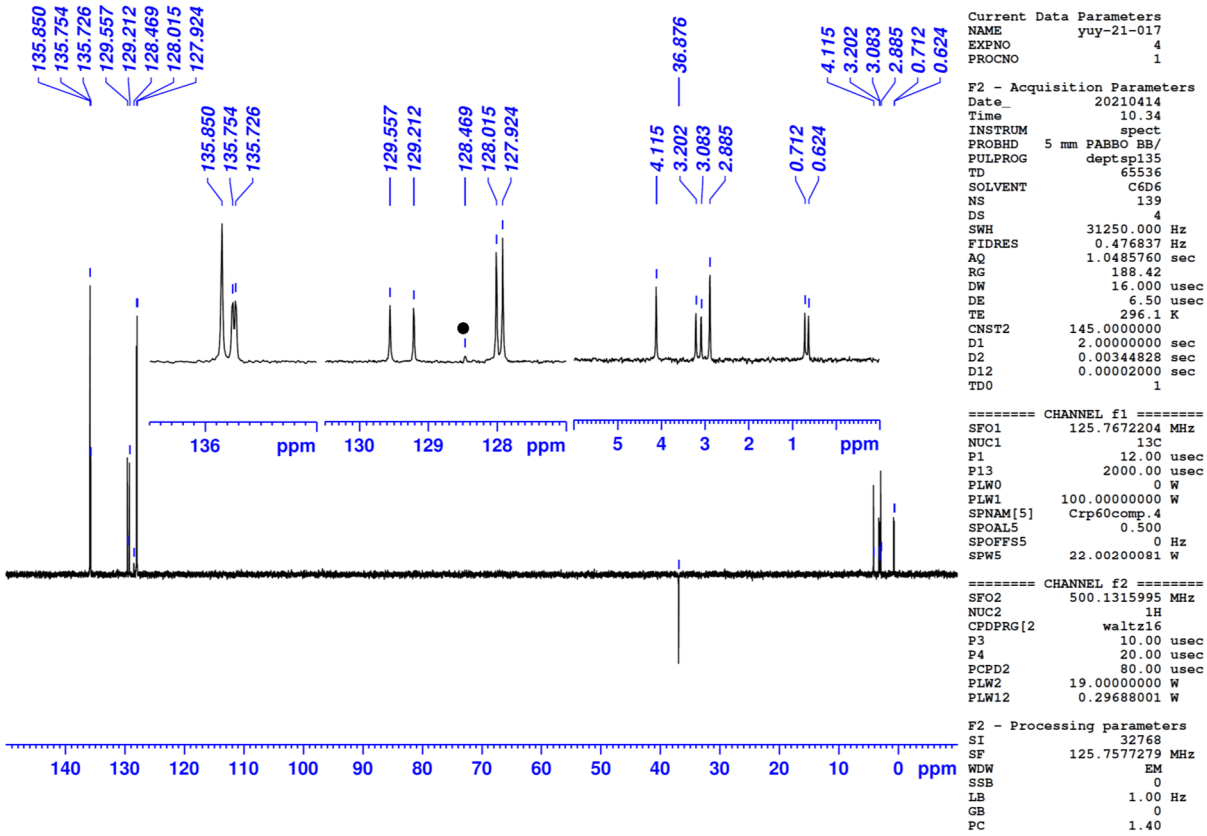

Fig. S4 $^{13}C\{^{1}H\}$ (DEPT135) NMR spectrum of **1** in C_6D_6 at 296 K (• = C_6HD_5).

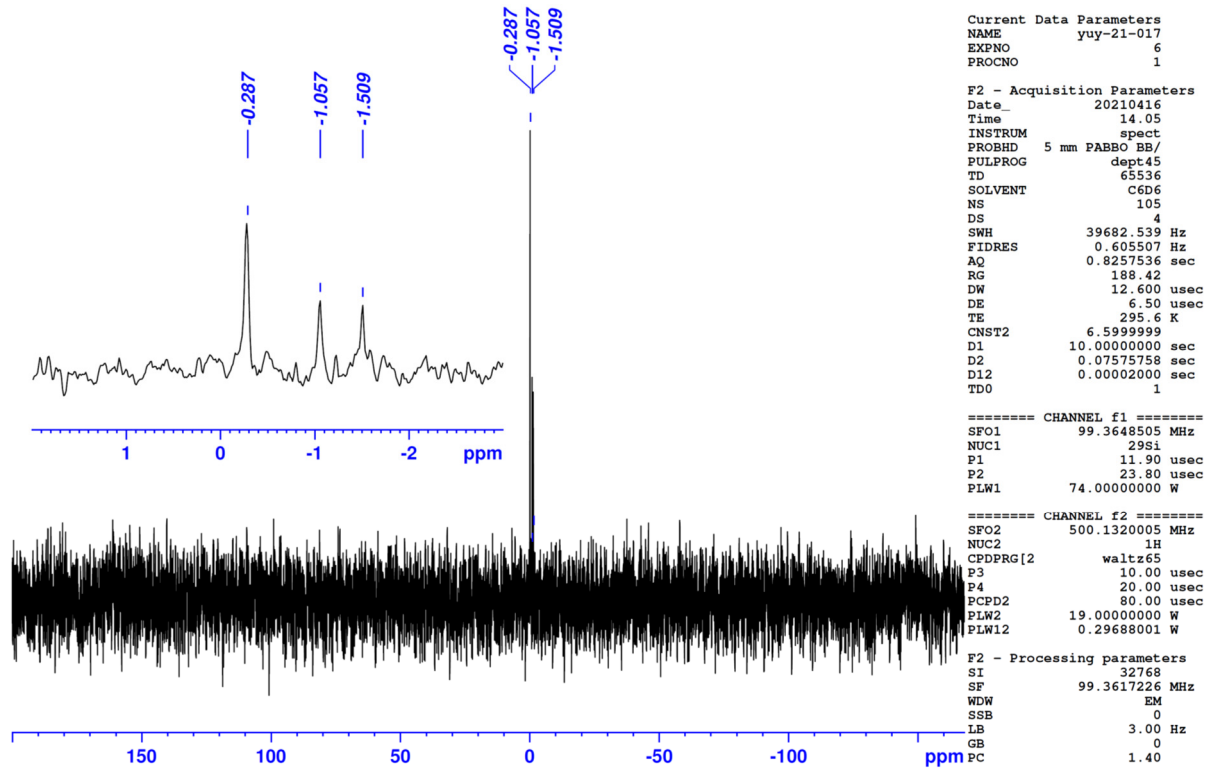

Fig. S5 $^{29}Si\{^{1}H\}$ (DEPT45) NMR spectrum of **1** in C_6D_6 at 296 K.

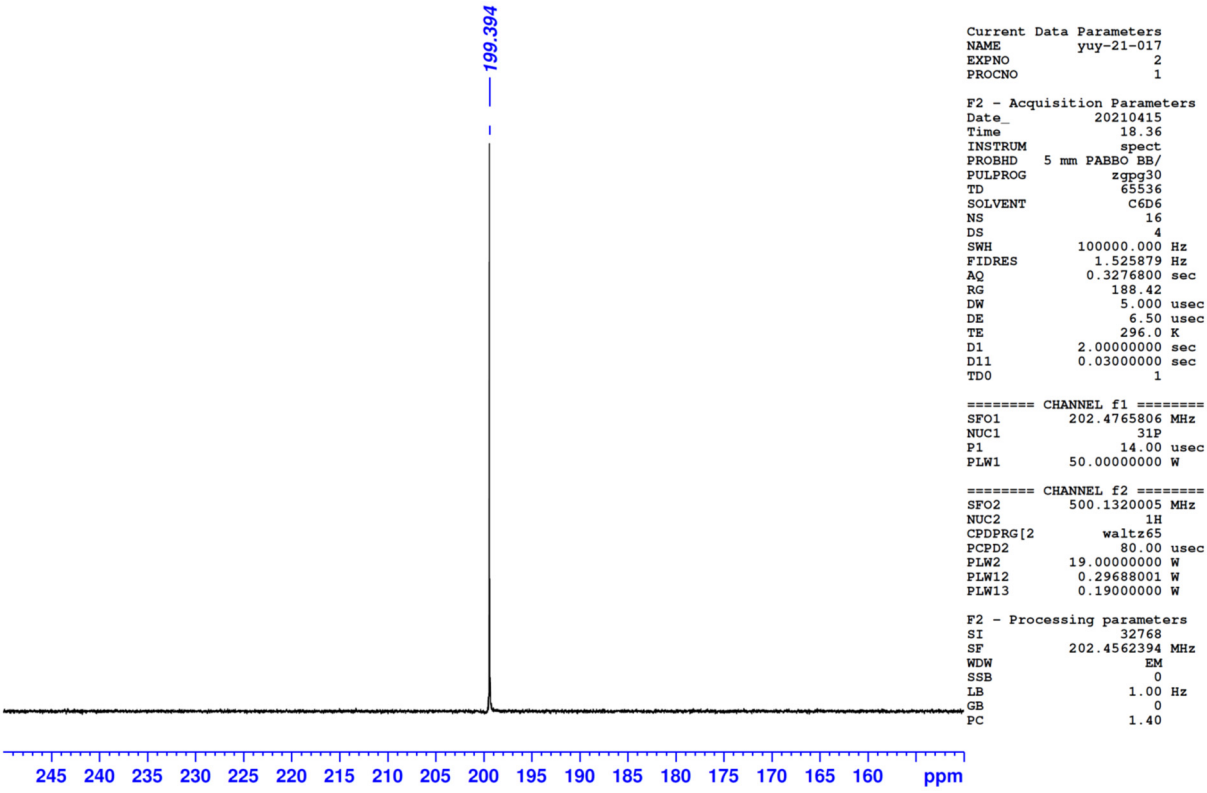

Fig. S6 $^{31}P\{^{1}H\}$ NMR spectrum of **1** in C_6D_6 at 296 K.

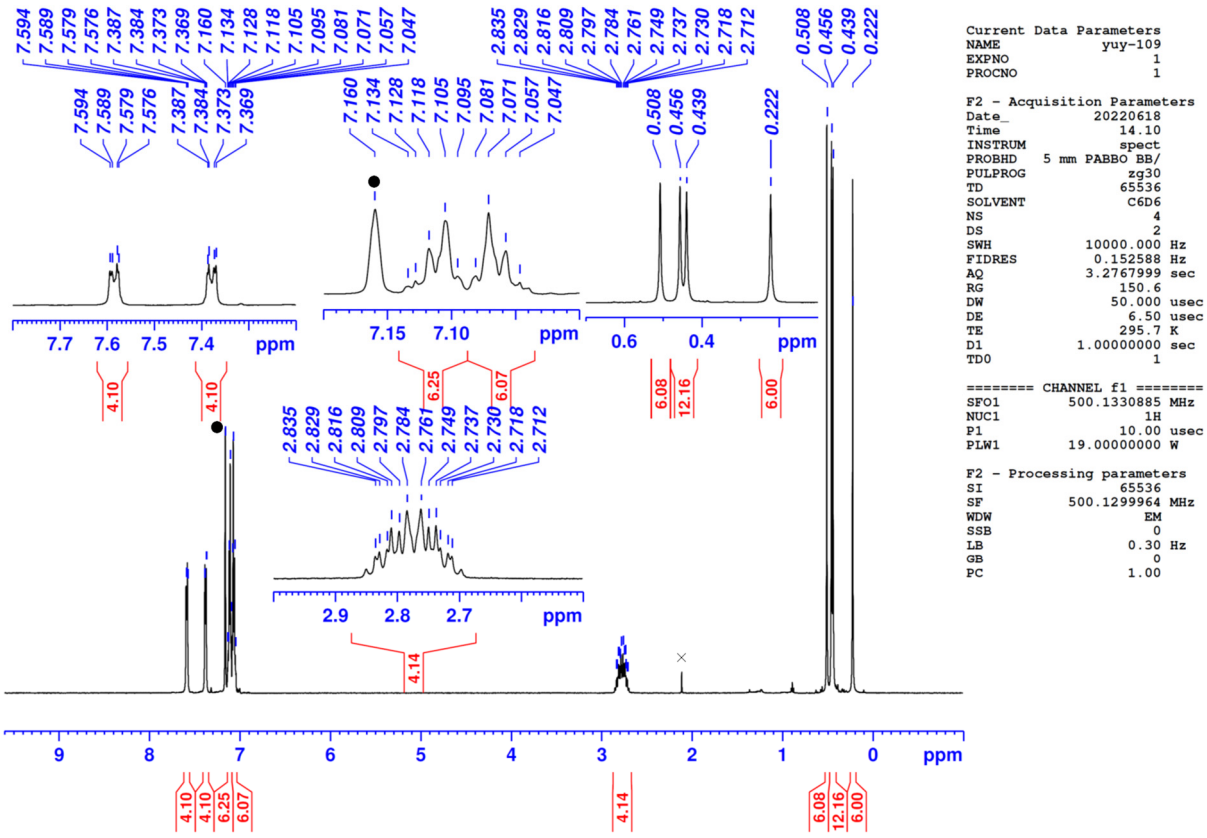

Fig. S7 ^{1}H NMR spectrum of **2** in C_6D_6 at 296 K (• = C_6HD_5, × = toluene).

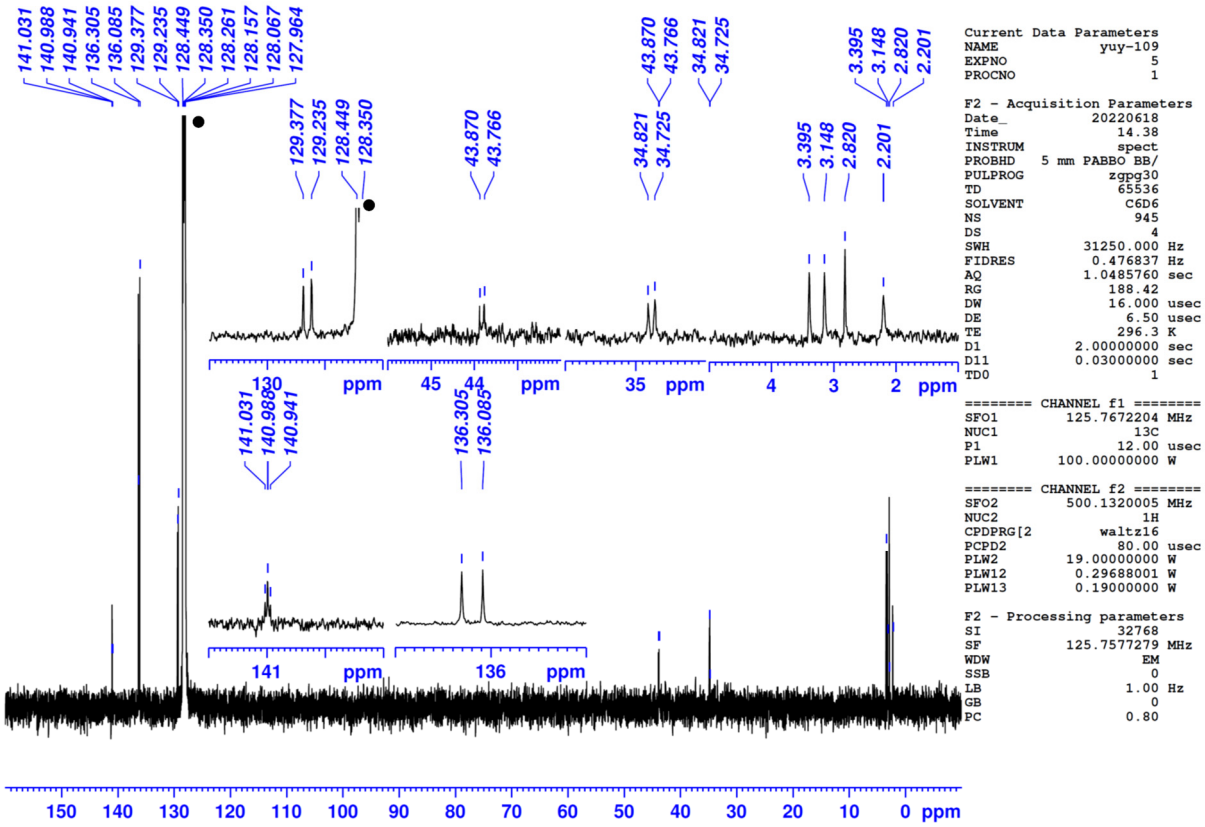

Fig. S8 $^{13}C\{^{1}H\}$ NMR spectrum of **2** in C_6D_6 at 296 K (• = C_6D_6).

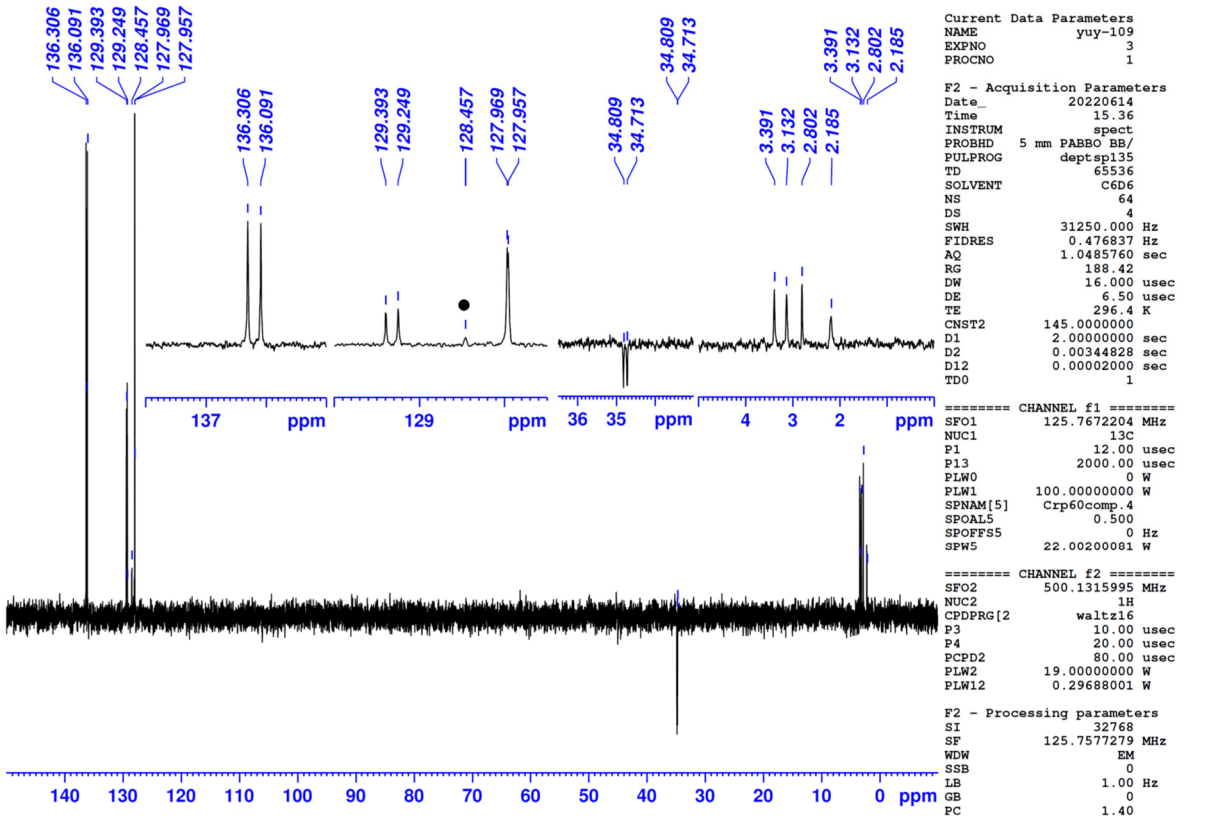

Fig. S9 $^{13}C\{^{1}H\}$ (dept135) NMR spectrum of **2** in C_6D_6 at 296 K (• = C_6HD_5).

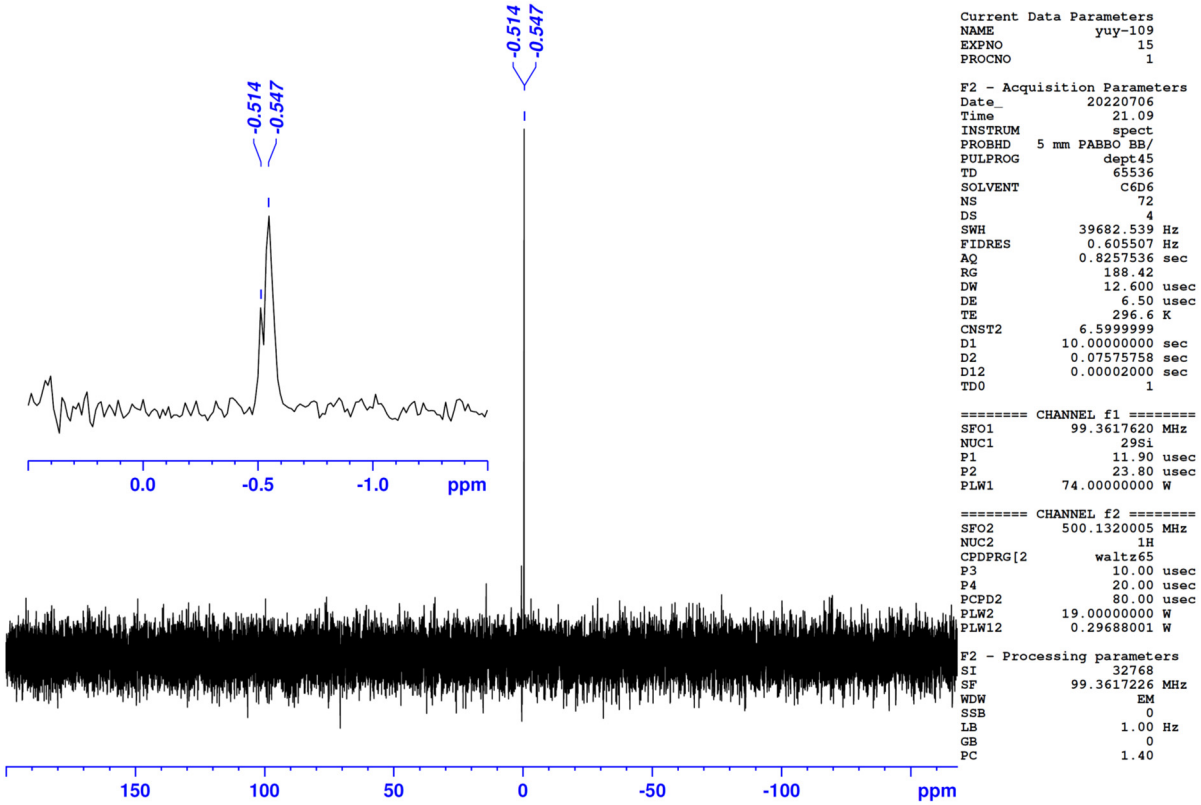

Fig. S10 $^{29}Si\{^{1}H\}$ (dept45) NMR spectrum of **2** in C_6D_6 at 297 K.

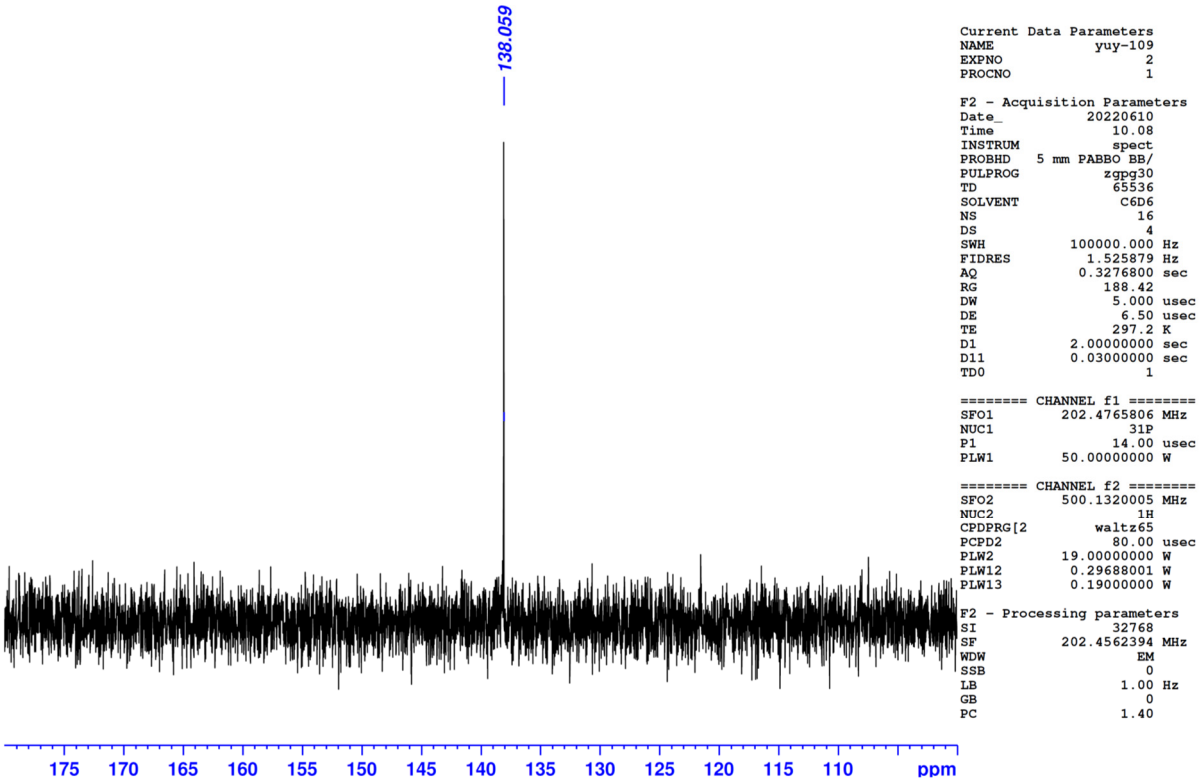

Fig. S11 $^{31}P\{^{1}H\}$ NMR spectrum of **2** in C_6D_6 at 297 K.

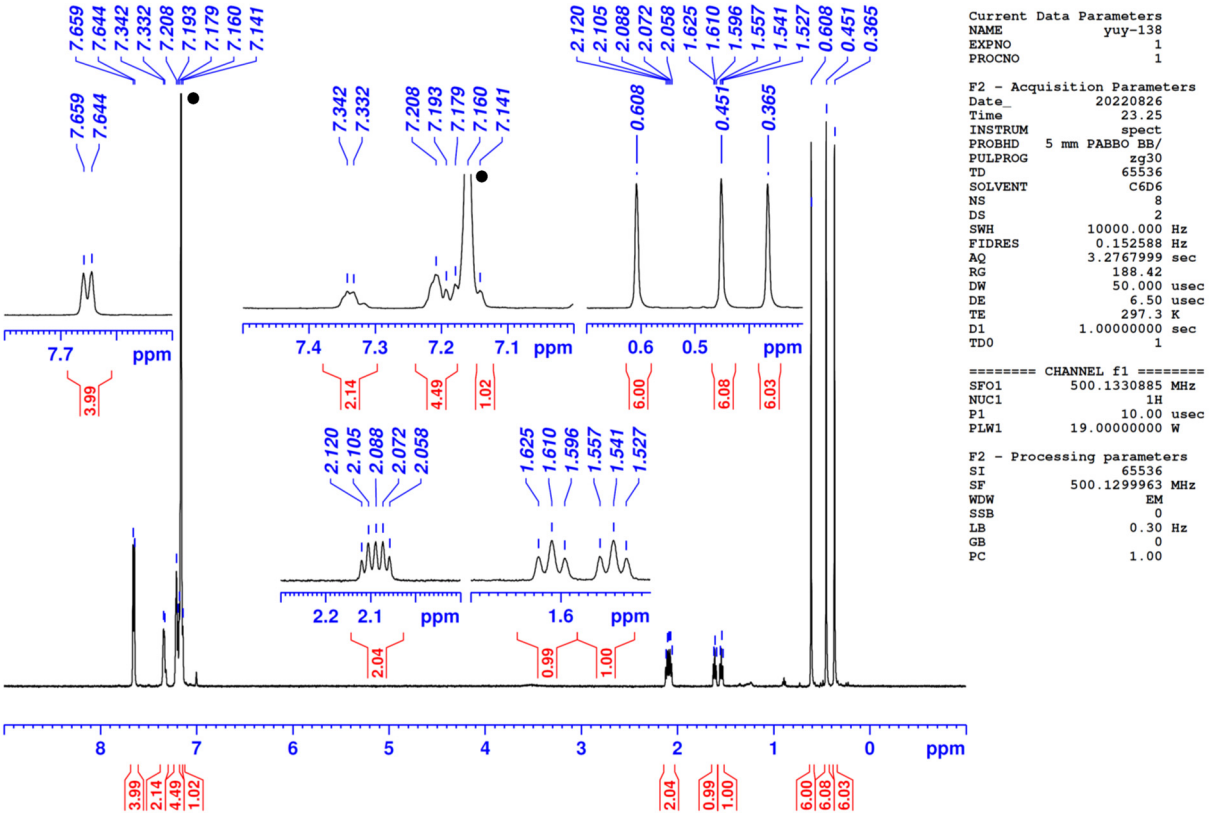

Fig. S12 ^{1}H NMR spectrum of **3** in C_6D_6 at 297 K (• = C_6HD_5).

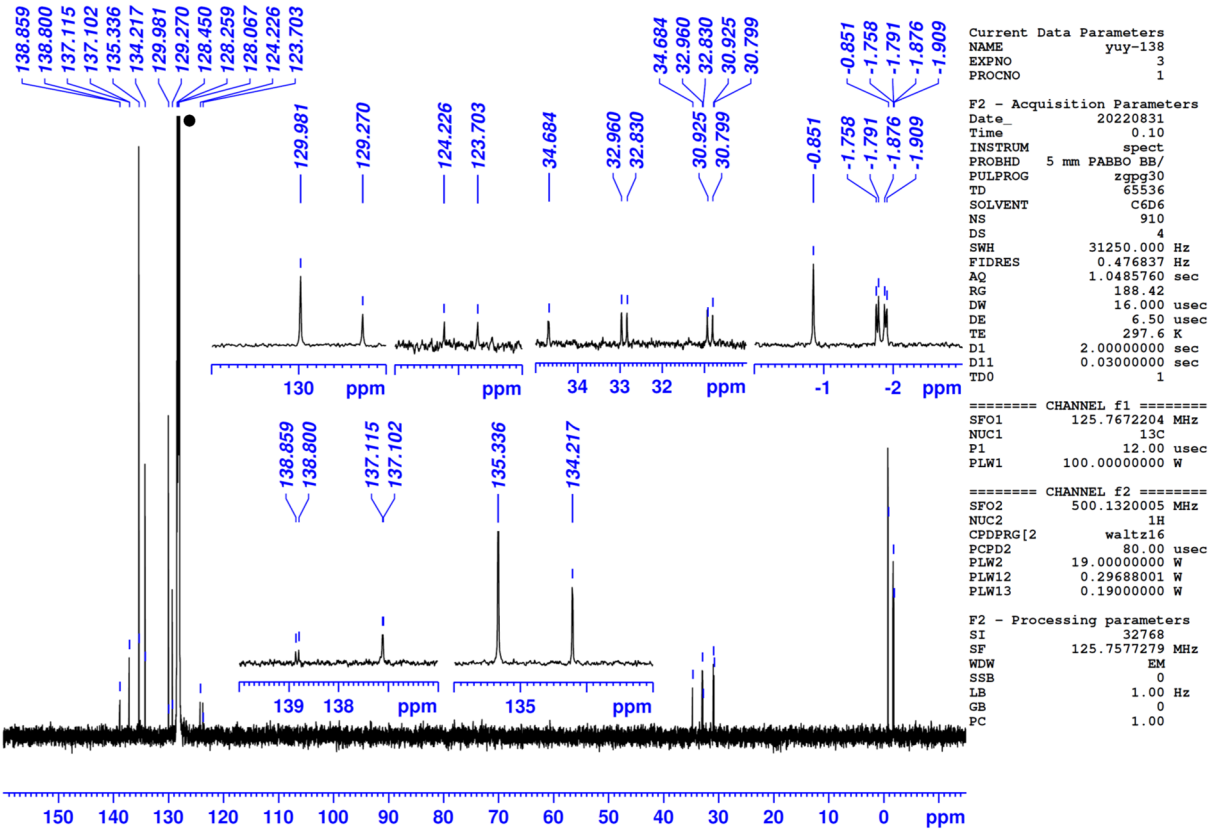

Fig. S13 ^{13}C{^{1}H} NMR spectrum of **3** in C_6D_6 at 298 K (• = C_6D_6).

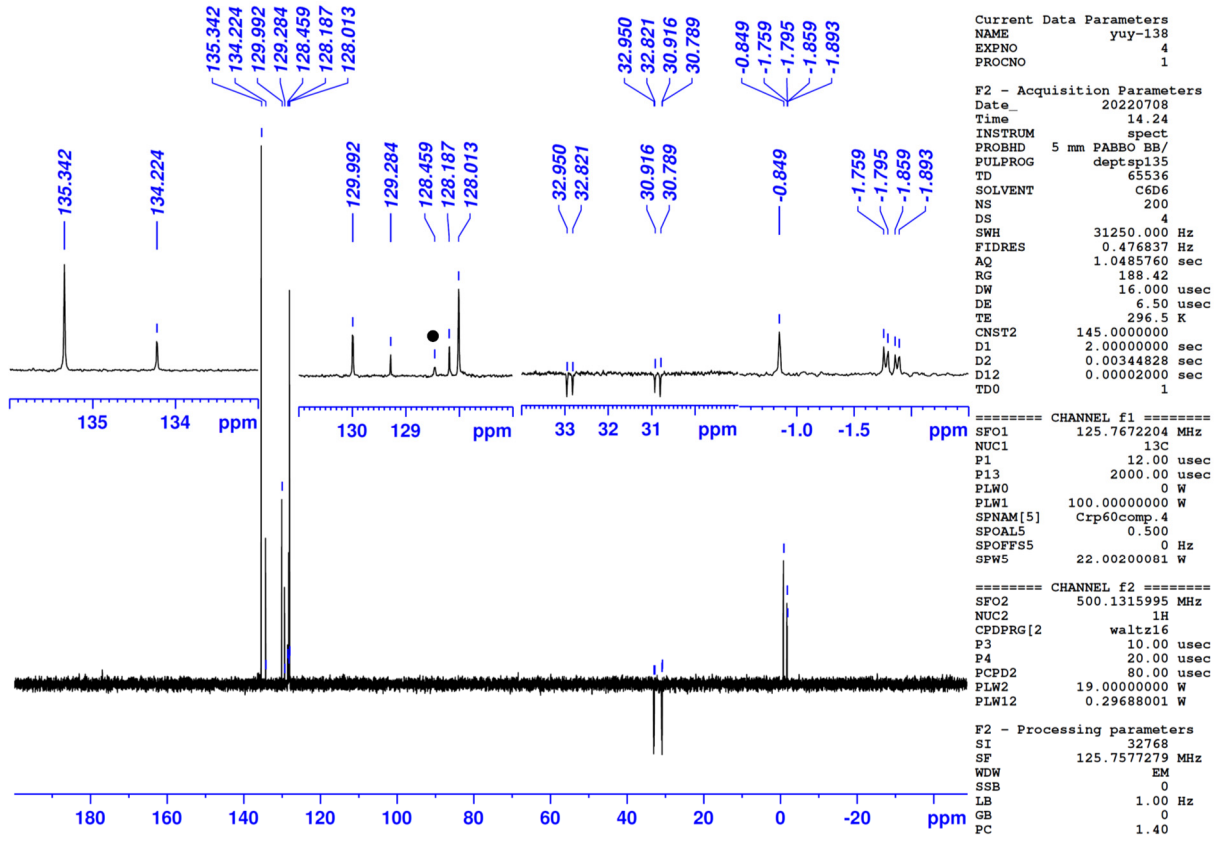

Fig. S14 $^{13}C\{^{1}H\}$ (dept135) NMR spectrum of **3** in C_6D_6 at 297 K (• = C_6HD_5).

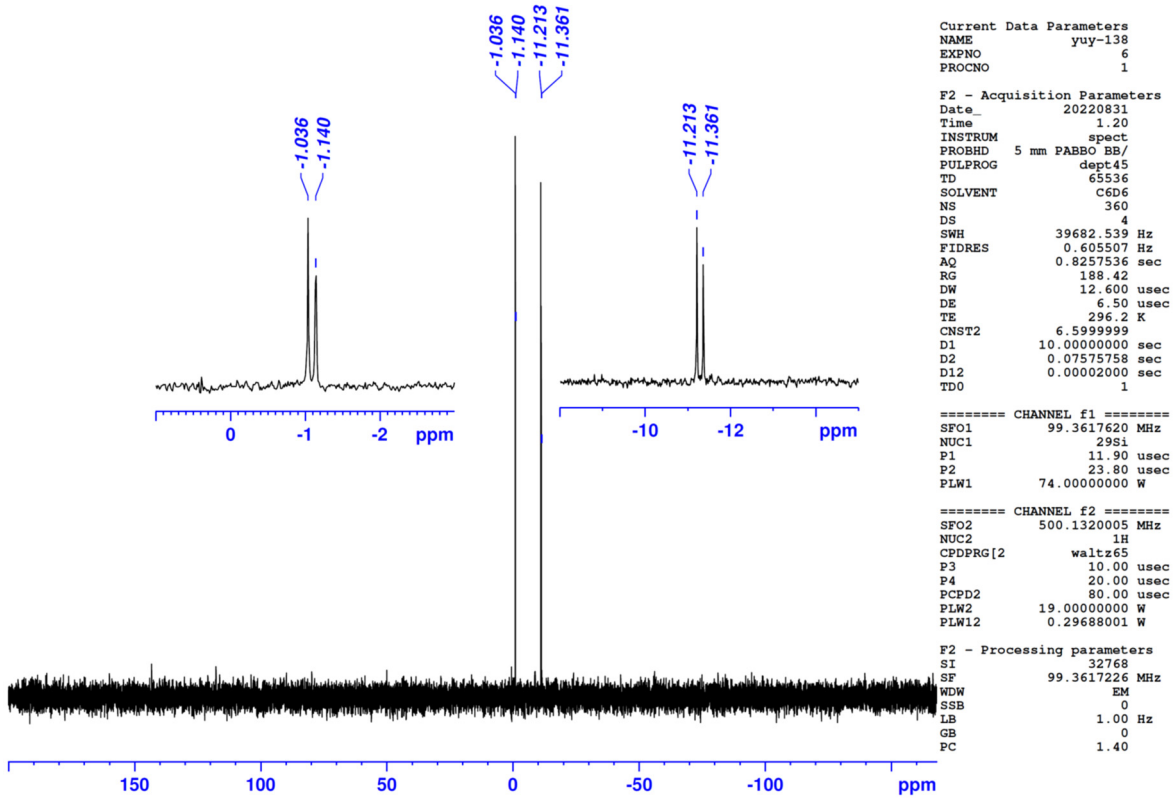

Fig. S15 $^{29}Si\{^{1}H\}$ (dept45) NMR spectrum of **3** in C_6D_6 at 296 K.

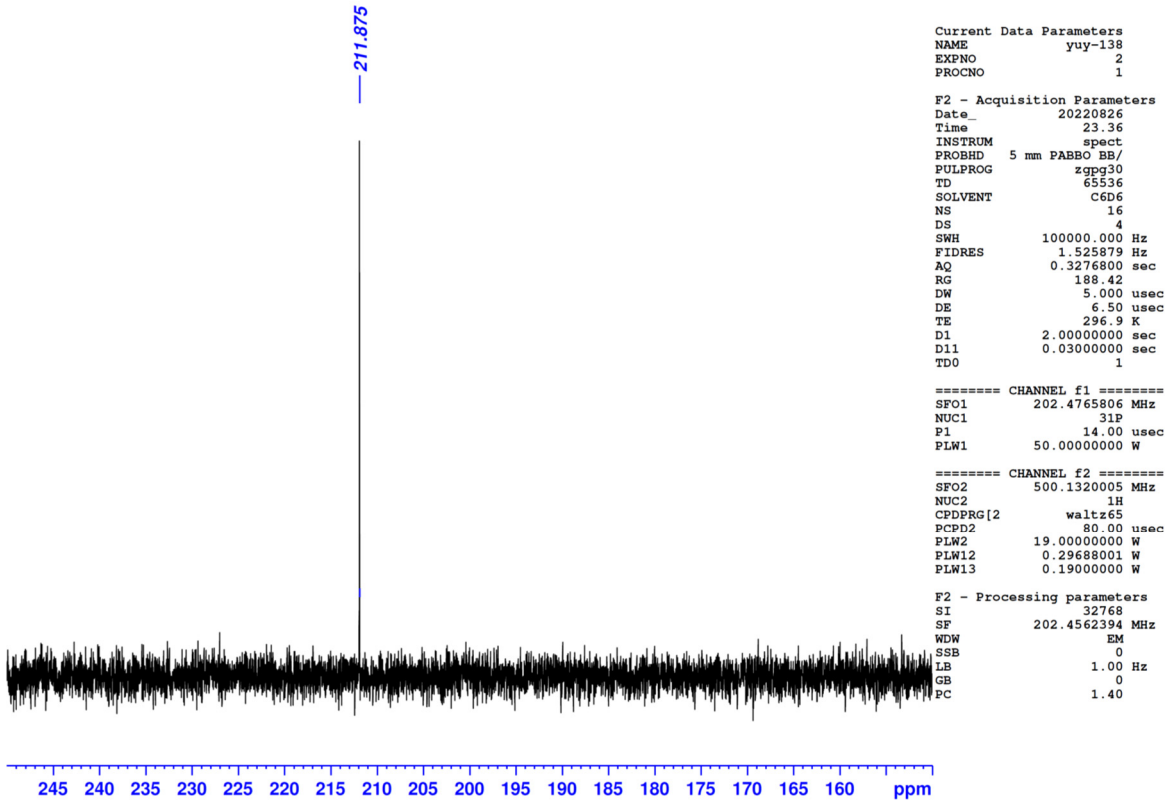

Fig. S16 $^{31}P\{^{1}H\}$ NMR spectrum of **3** in C_6D_6 at 297 K.

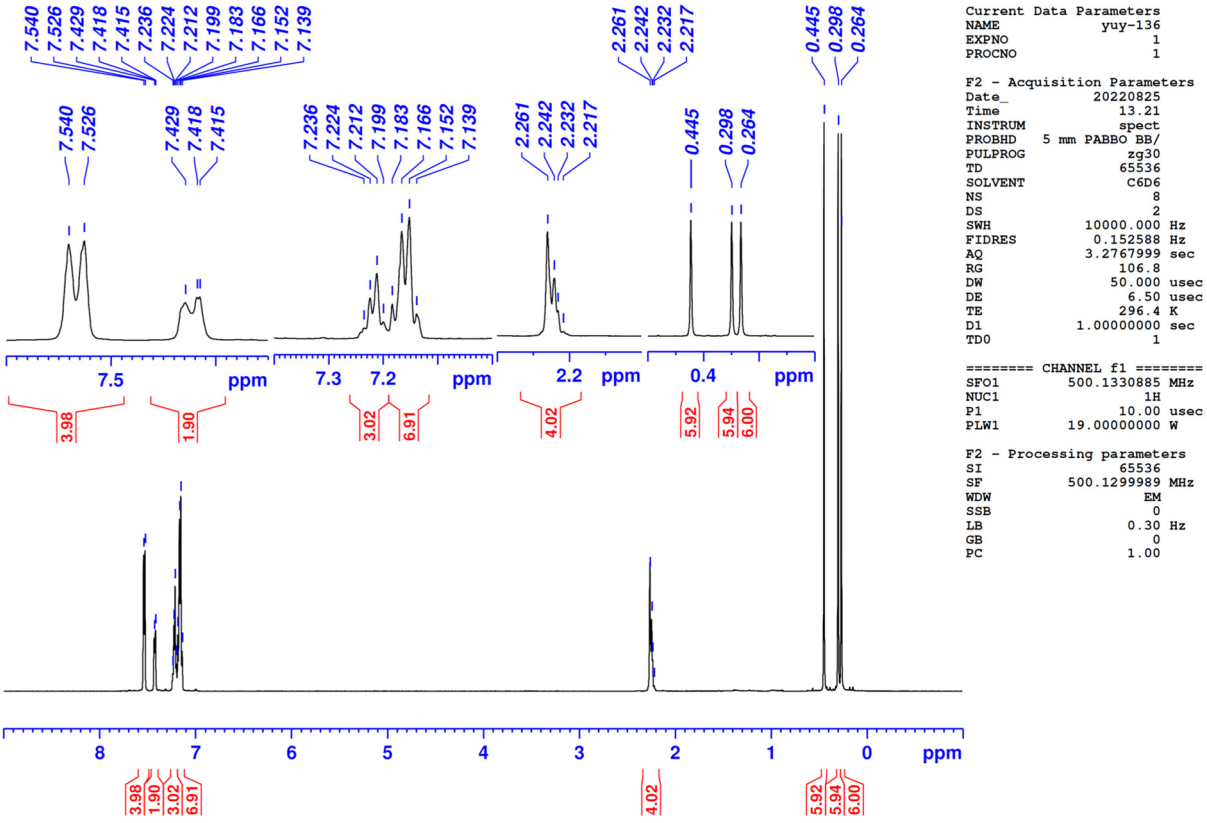

Fig. S17 ^{1}H NMR spectrum of **4** in C_6D_6 at 296 K.

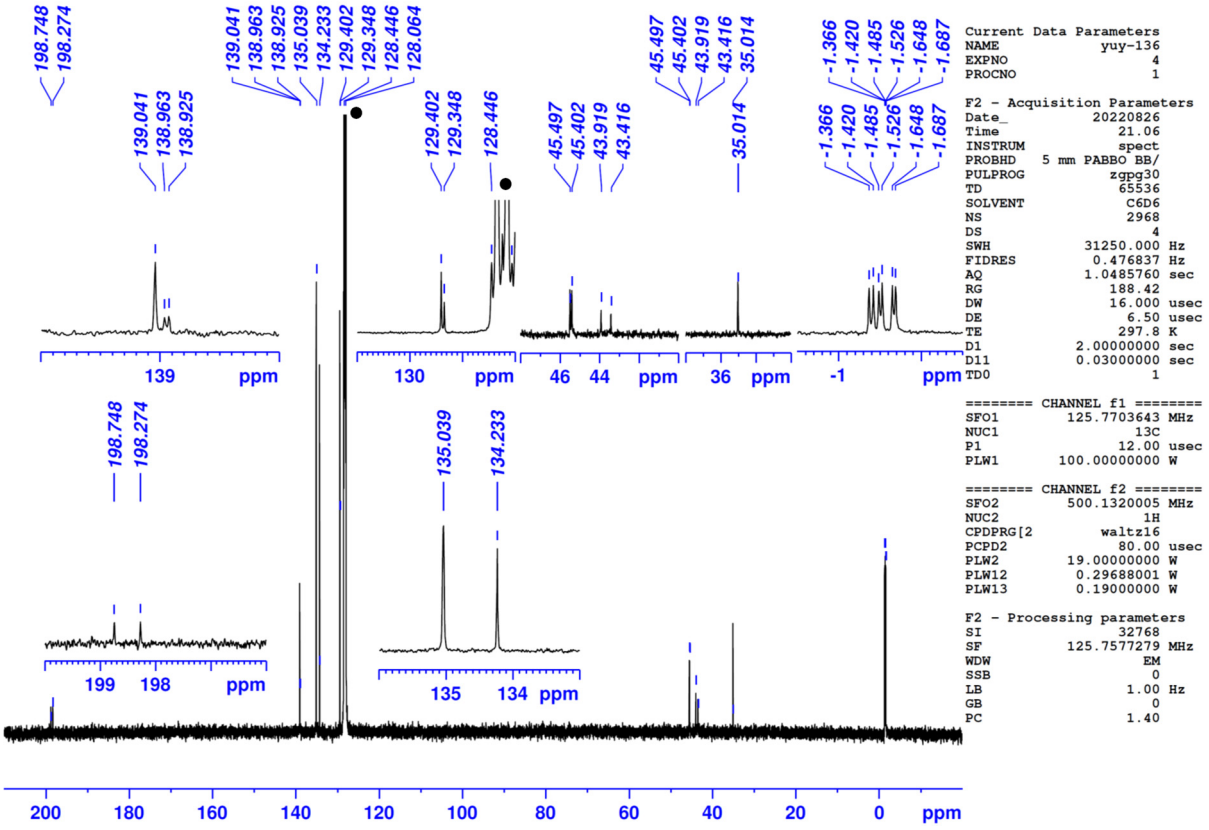

Fig. S18 $^{13}C\{^{1}H\}$ NMR spectrum of **4** in C_6D_6 at 298 K (• = C_6D_6).

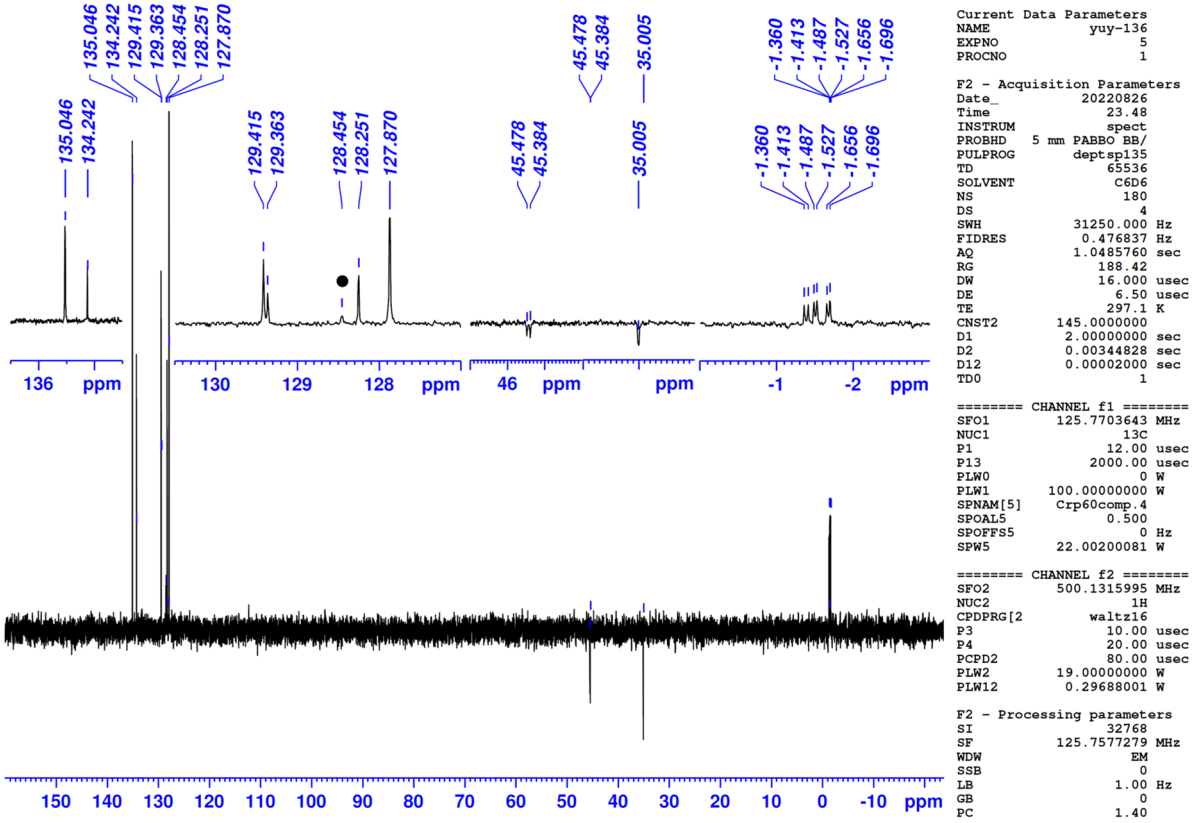

Fig. S19 $^{13}C\{^{1}H\}$ (dept135) NMR spectrum of **4** in C_6D_6 at 297 K (• = C_6HD_5).

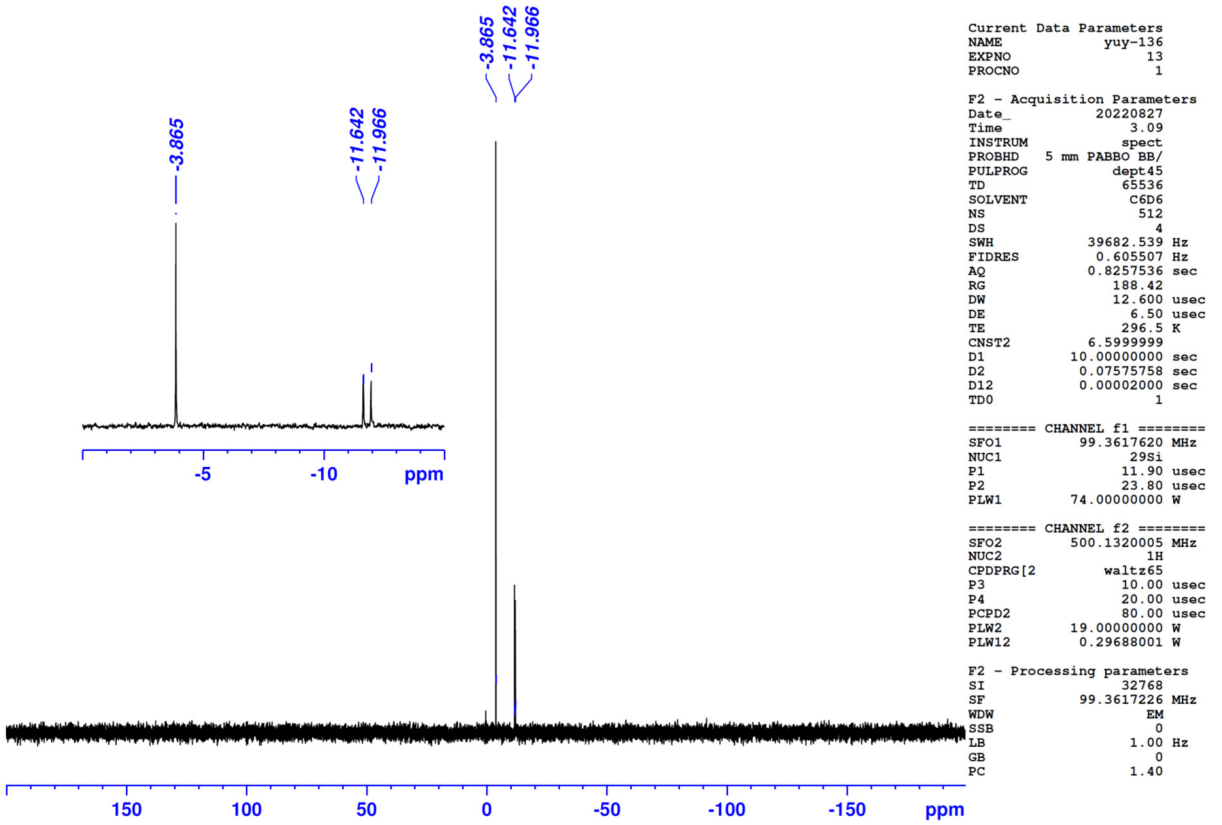

Fig. S20 $^{29}Si\{^{1}H\}$ (dept45) NMR spectrum of **4** in C_6D_6 at 297 K.

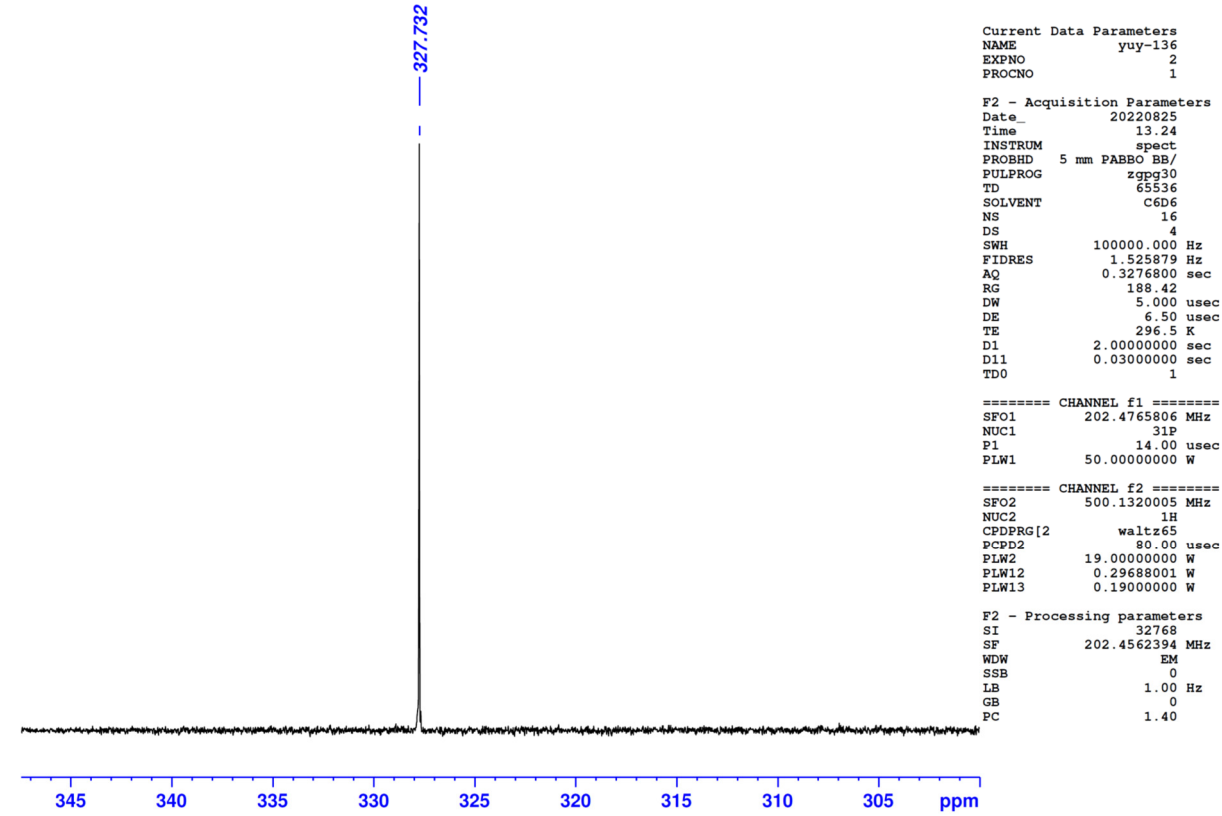

Fig. S21 $^{31}P\{^{1}H\}$ NMR spectrum of **4** in C_6D_6 at 297 K.

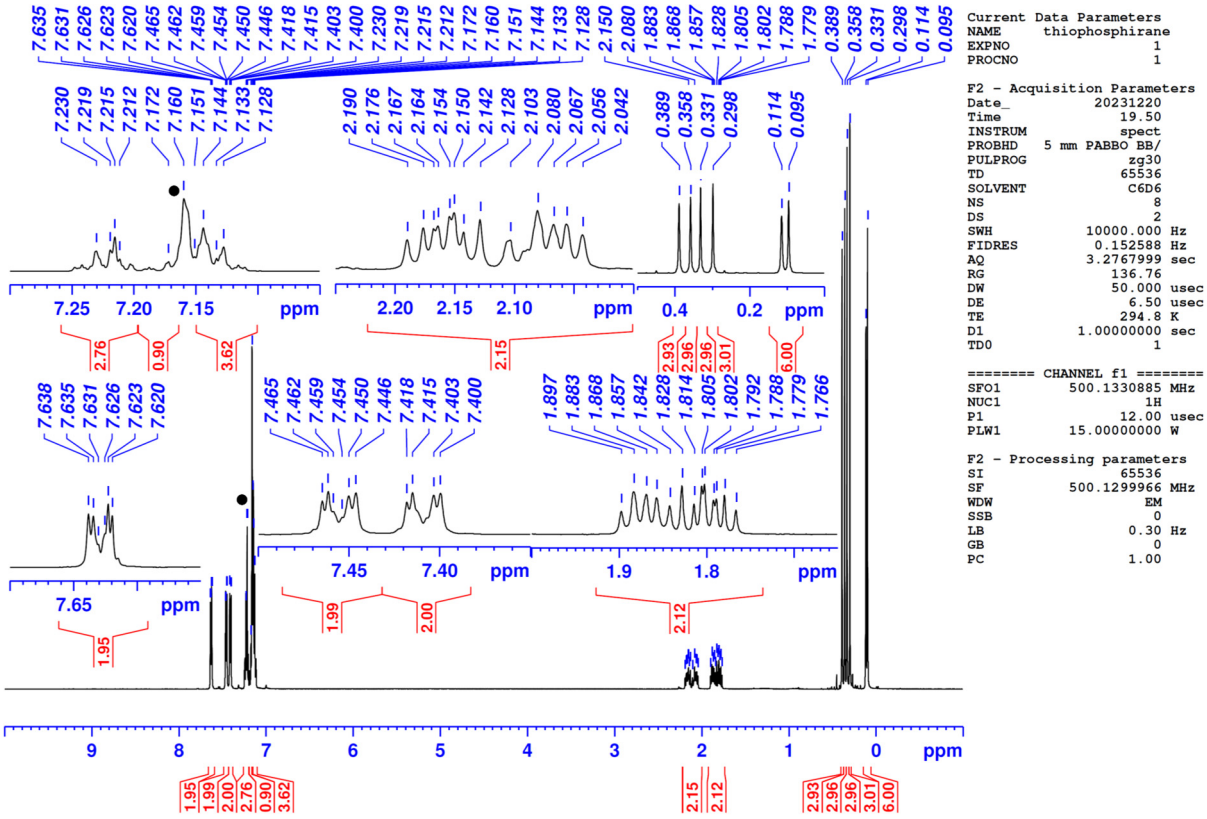

Fig. S22 ^{1}H NMR spectrum of **5** in C_6D_6 at 295 K (• = C_6HD_5).

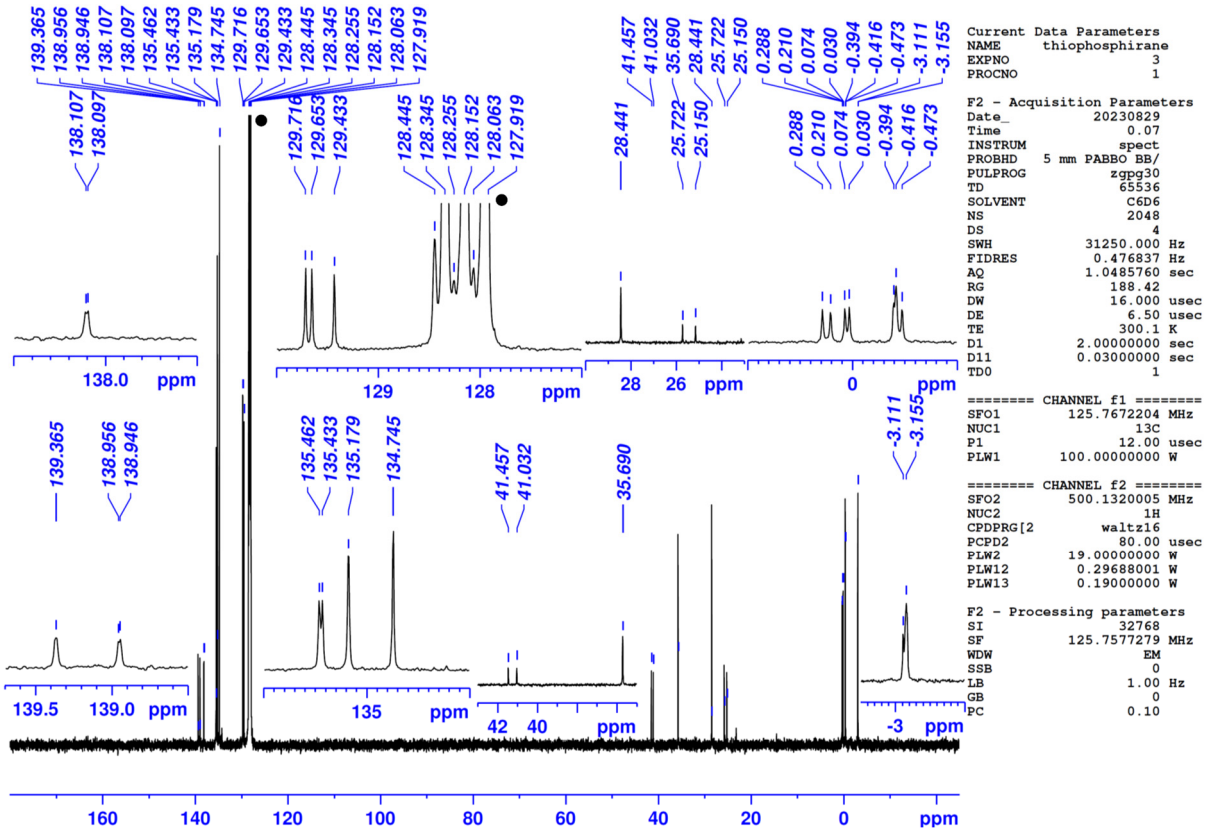

Fig. S23 $^{13}C\{^{1}H\}$ NMR spectrum of **5** in C_6D_6 at 300 K (• = C_6D_6).

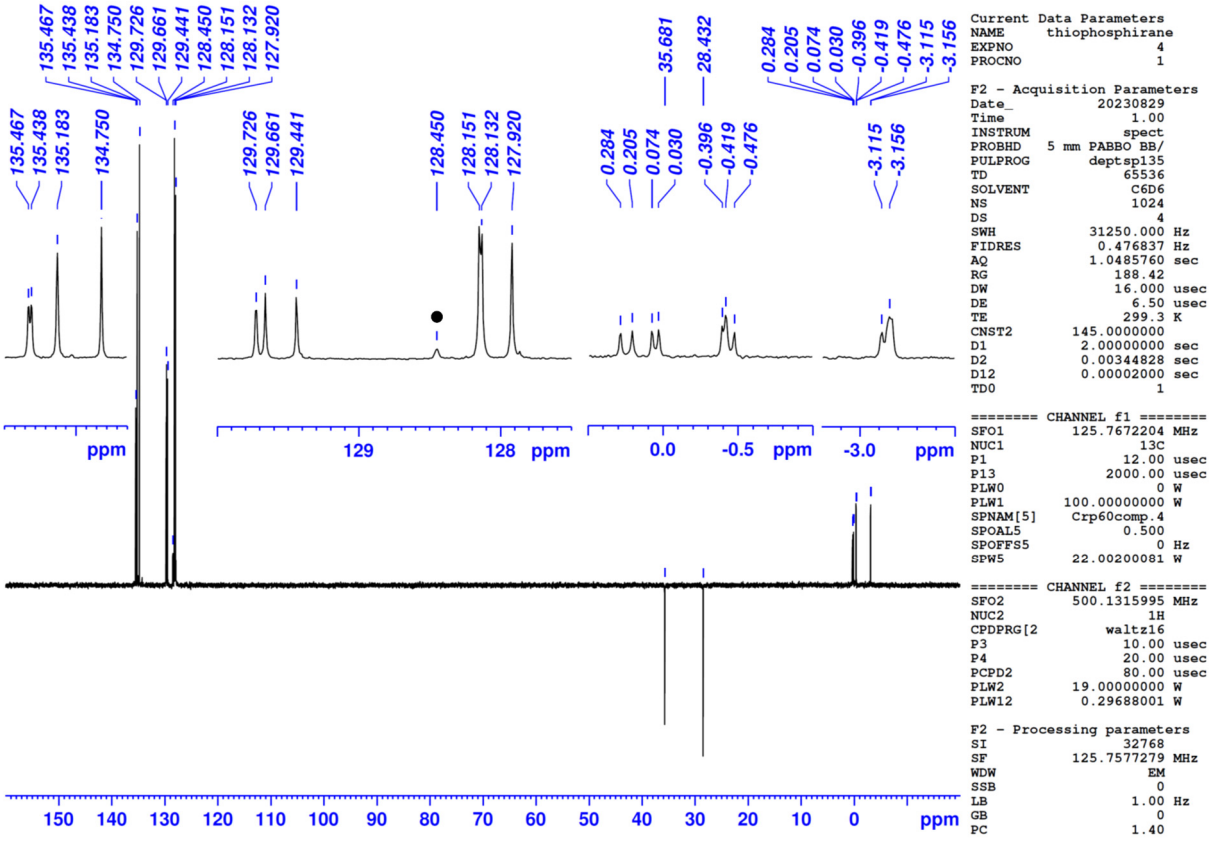

Fig. S24 $^{13}C\{^{1}H\}$ (dept135) NMR spectrum of **5** in C_6D_6 at 299 K (• = C_6HD_5).

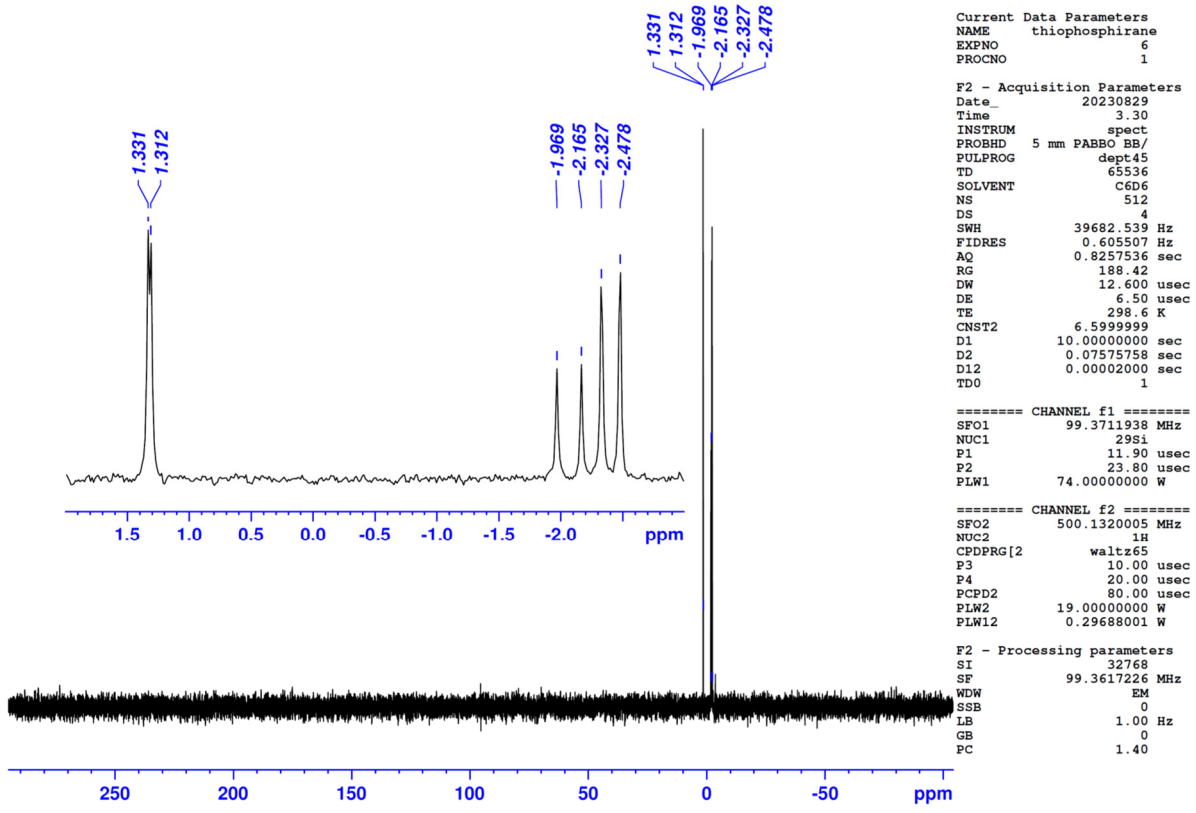

Fig. S25 $^{29}Si\{^{1}H\}$ (dept45) NMR spectrum of **5** in C_6D_6 at 299 K.

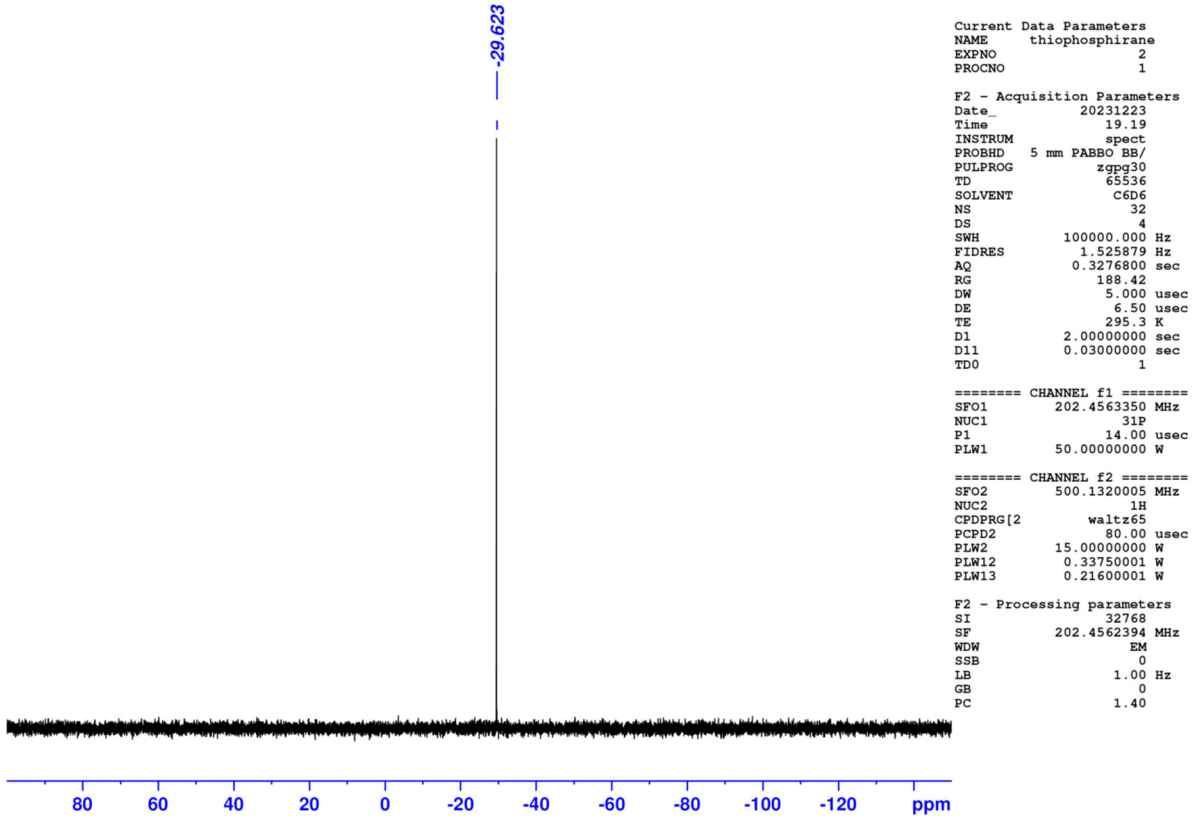

Fig. S26 $^{31}P\{^{1}H\}$ NMR spectrum of **5** in C_6D_6 at 295 K.

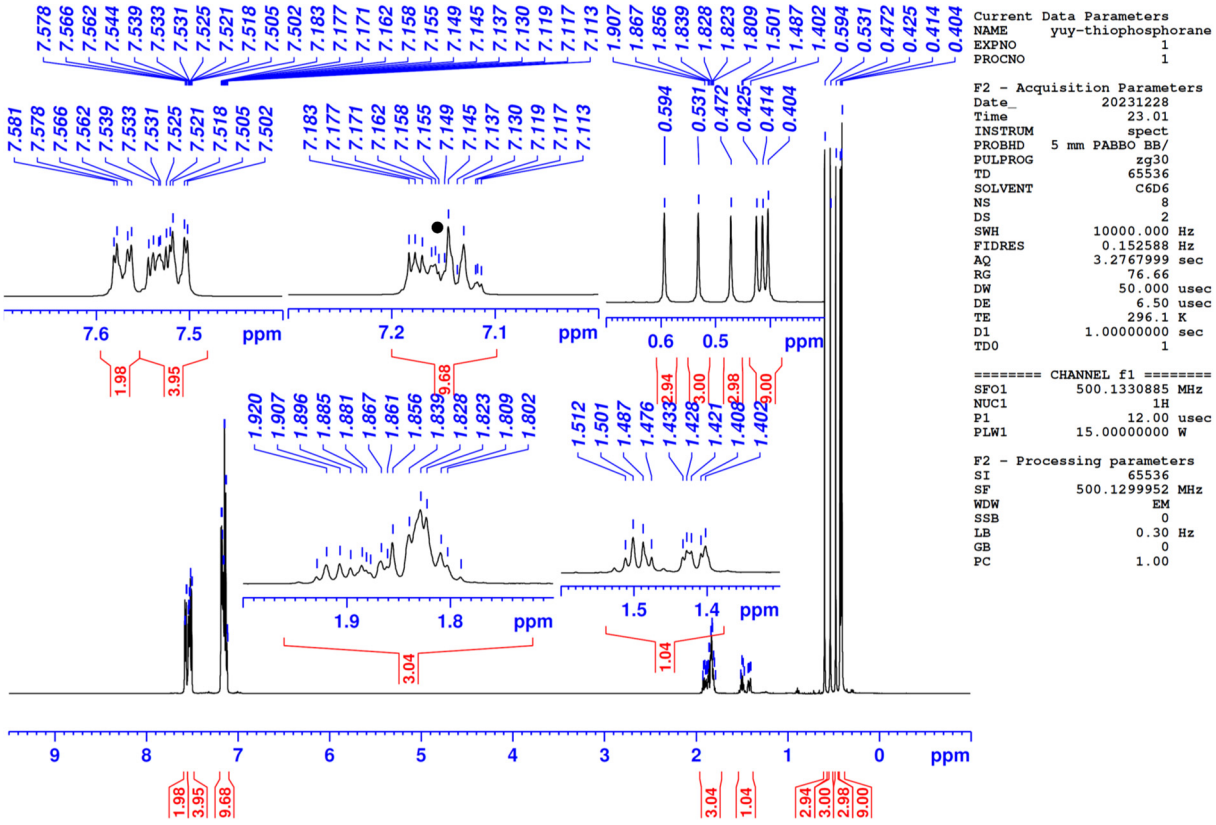

Fig. S27 ^{1}H NMR spectrum of **6** in C_6D_6 at 296 K (• = C_6HD_5).

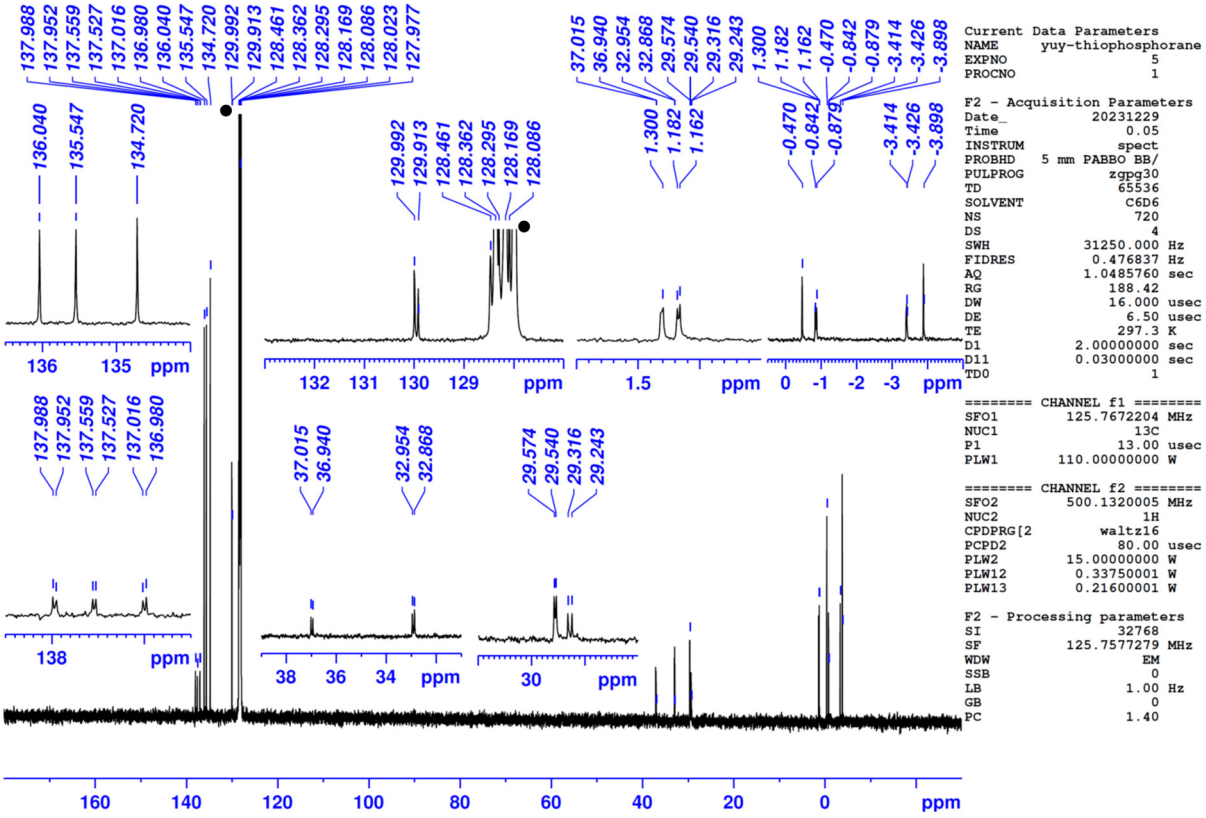

Fig. S28 $^{13}C\{^{1}H\}$ NMR spectrum of **6** in C_6D_6 at 297 K (• = C_6D_6).

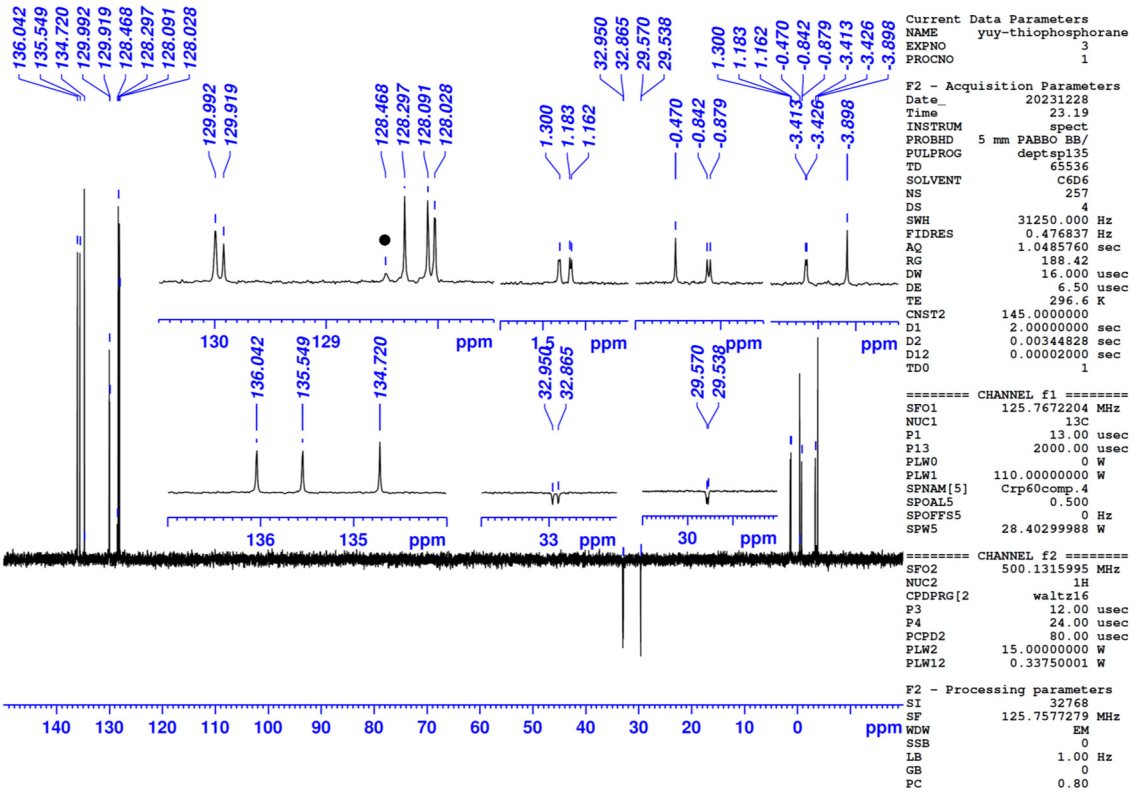

Fig. S29 $^{13}C\{^{1}H\}$ (dept135) NMR spectrum of **6** in C_6D_6 at 297 K (• = C_6HD_5).

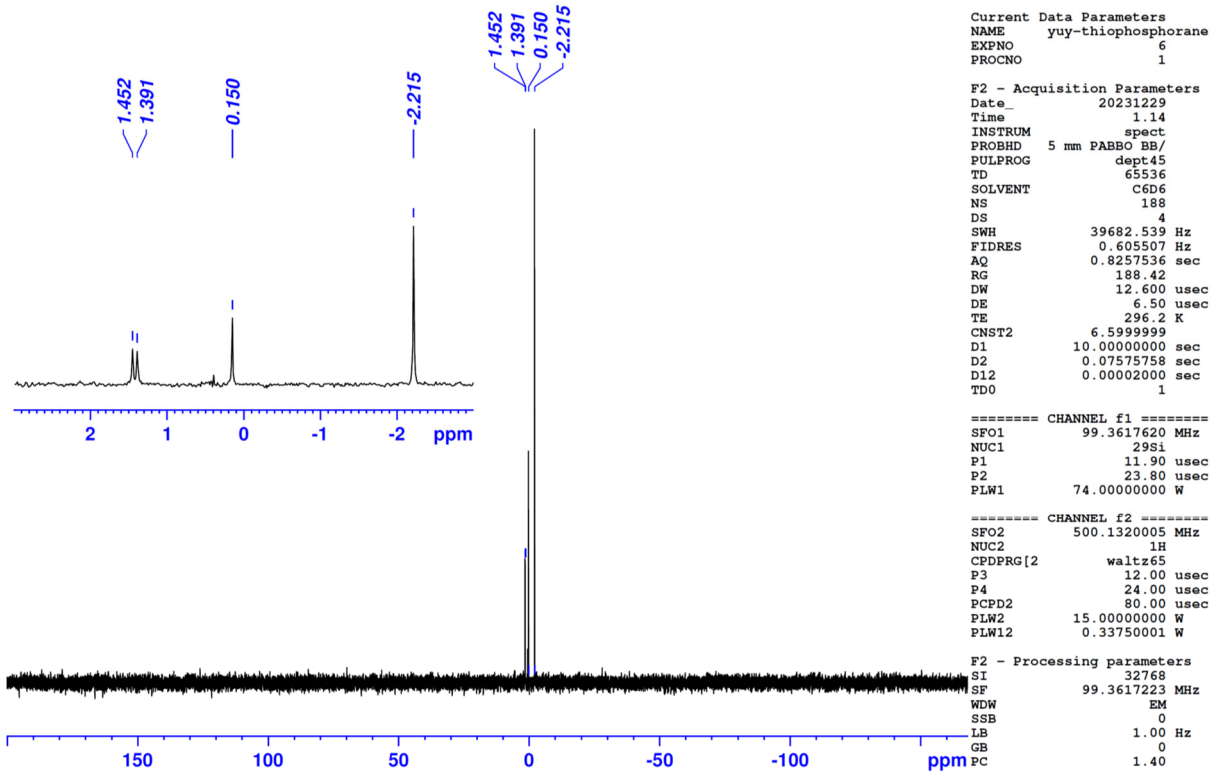

Fig. S30 $^{29}Si\{^{1}H\}$ (dept45) NMR spectrum of **6** in C_6D_6 at 296 K.

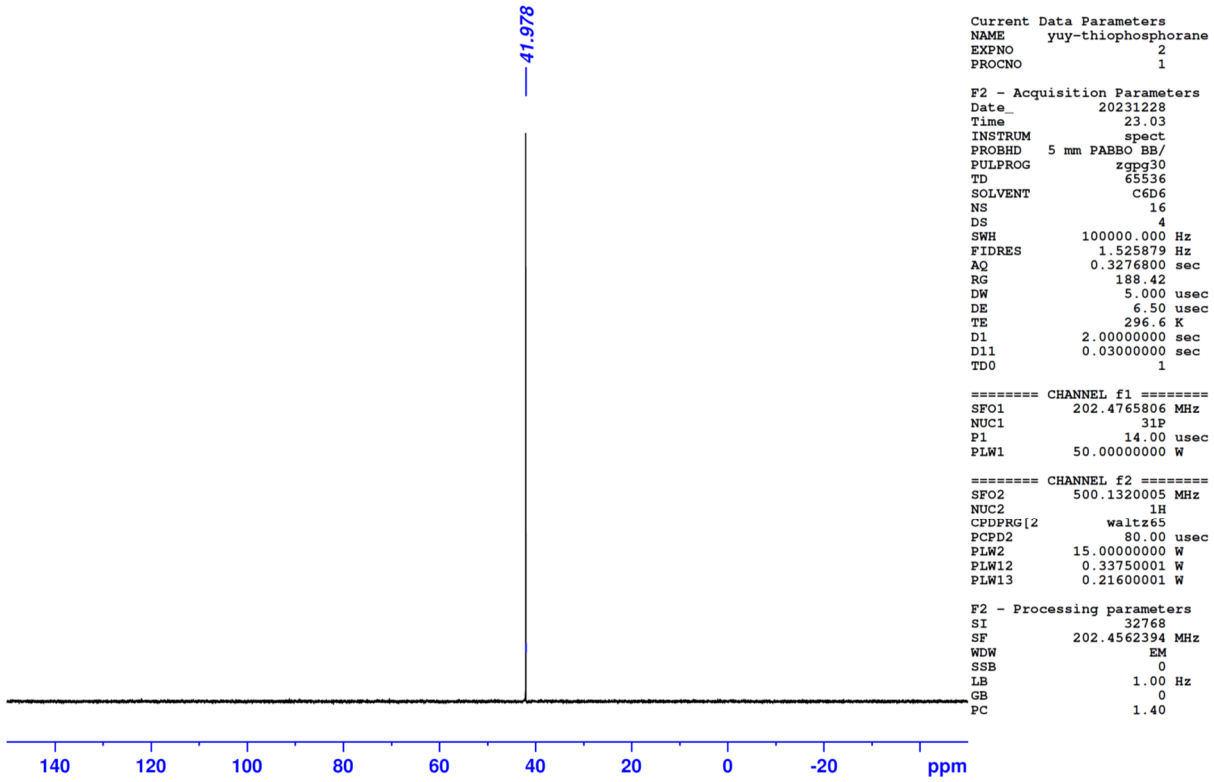

Fig. S31 $^{31}P\{^{1}H\}$ NMR spectrum of **6** in C_6D_6 at 297 K.

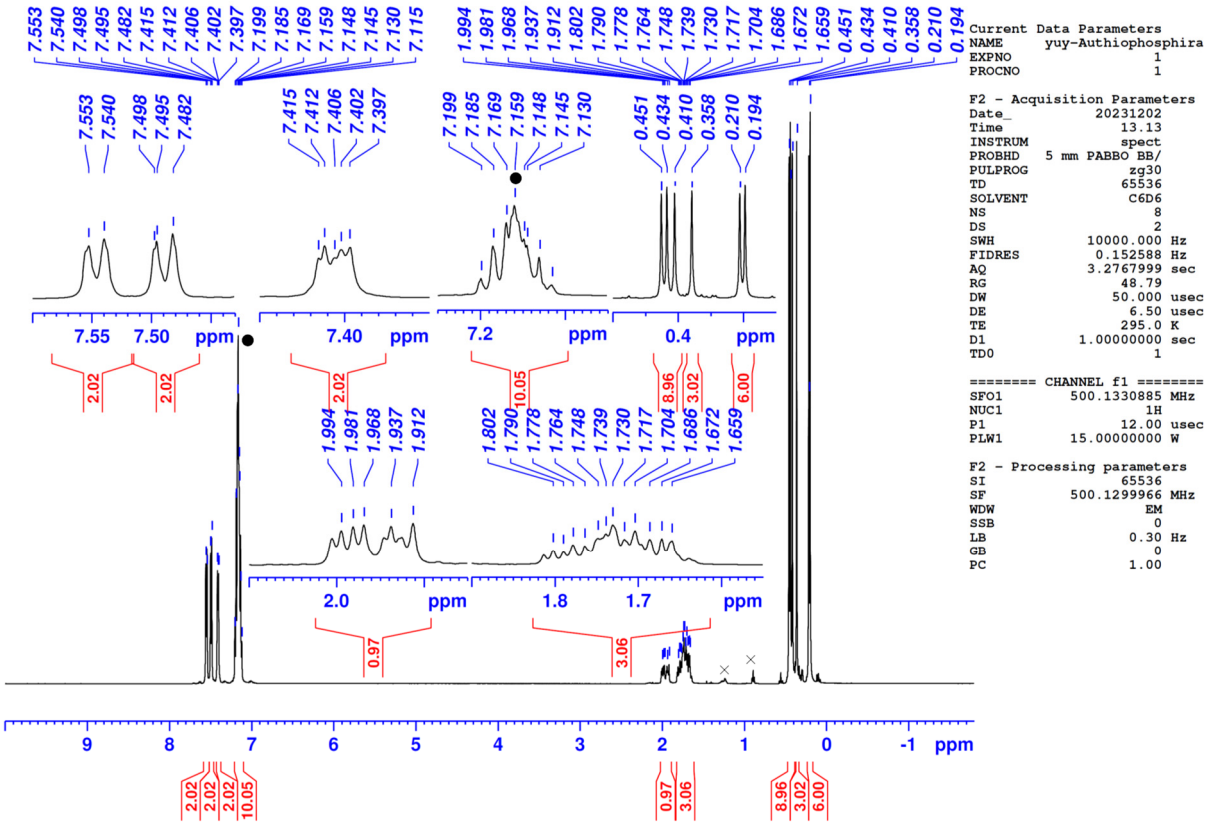

Fig. S32 ^{1}H NMR spectrum of **5Au** in C_6D_6 at 295 K (• = C_6HD_5, × = hexane).

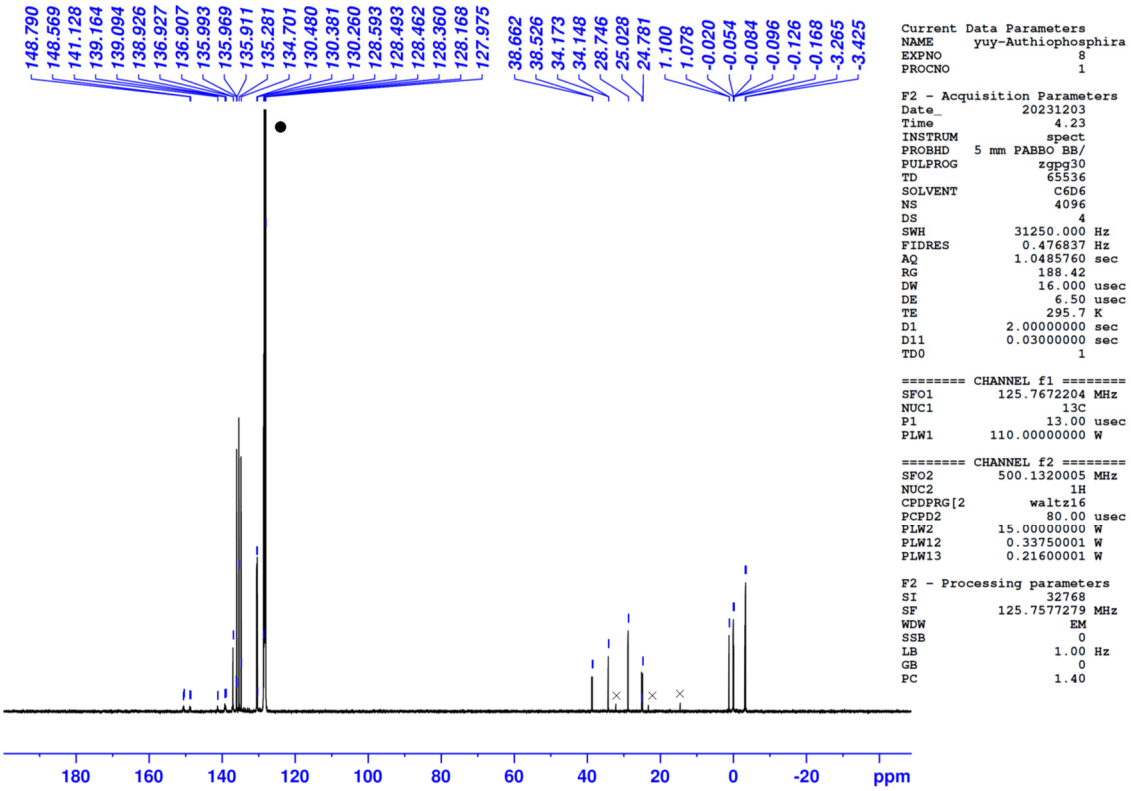

Fig. S33 ^{13}C {^{1}H} NMR spectrum of **5Au** in C_6D_6 at 296 K (• = C_6HD_5, × = hexane).

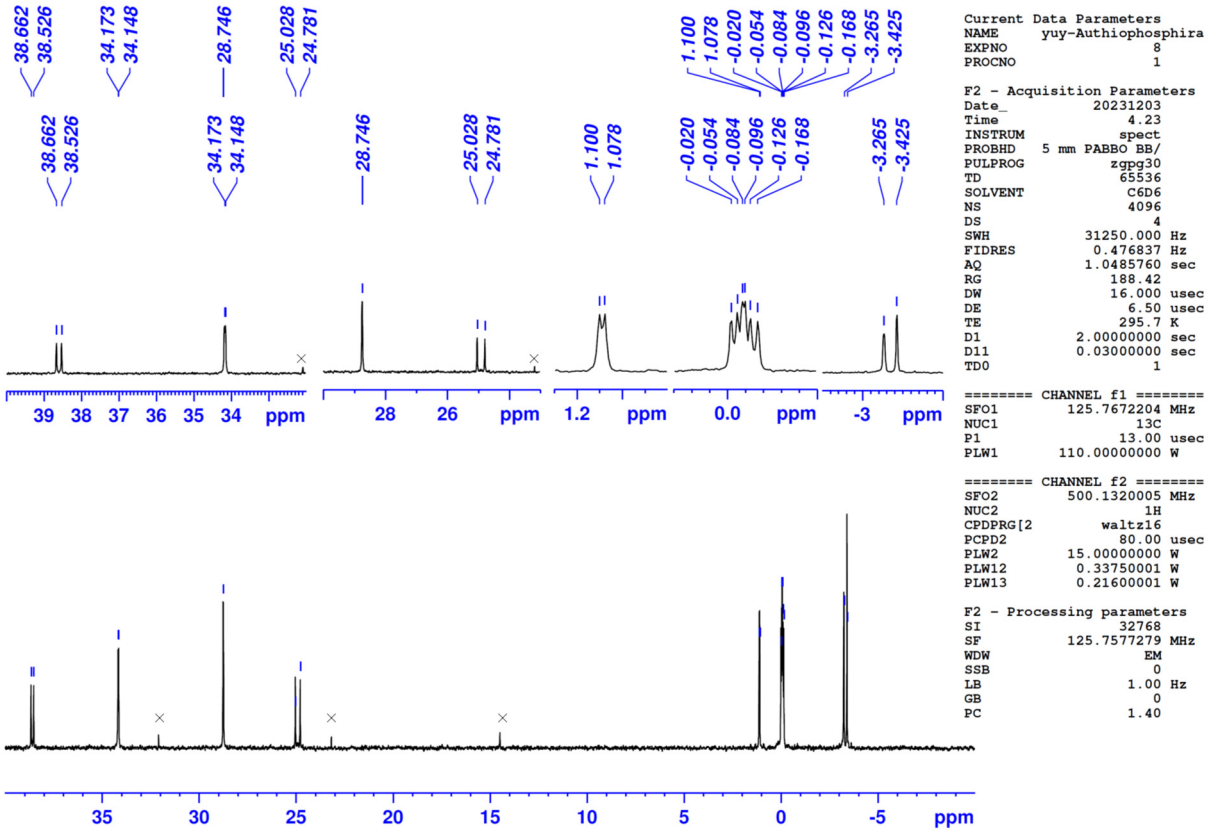

Fig. S34 ^{13}C {^{1}H} NMR spectrum of **5Au** (40 ppm to-10 ppm) in C_6D_6 at 296 K (• = C_6HD_5, × = hexane).

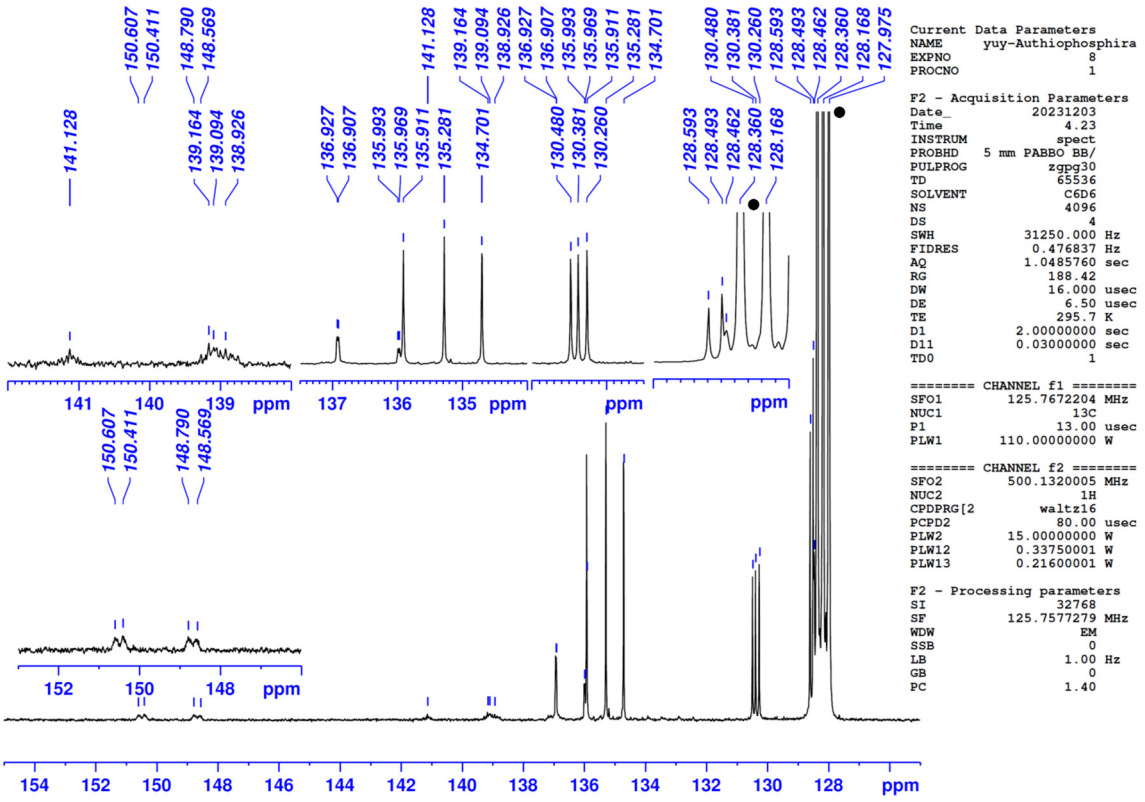

Fig. S35 ^{13}C {^{1}H} NMR spectrum of **5Au** (155 ppm to 125 ppm)) in C_6D_6 at 296 K (• = C_6HD_5, × =hexane).

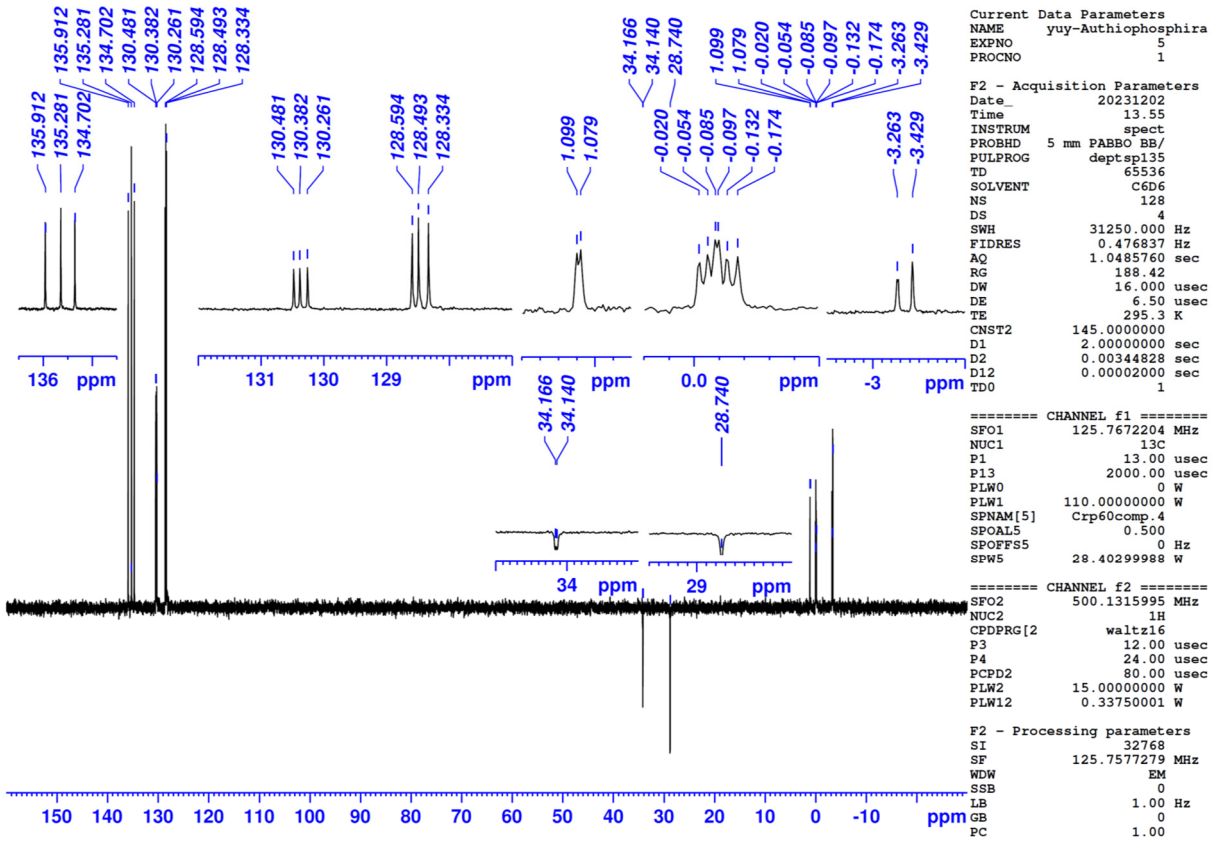

Fig. S36 ^{13}C {^{1}H} (dept135) NMR spectrum of **5Au** in C_6D_6 at 296 K (• = C_6HD_5).

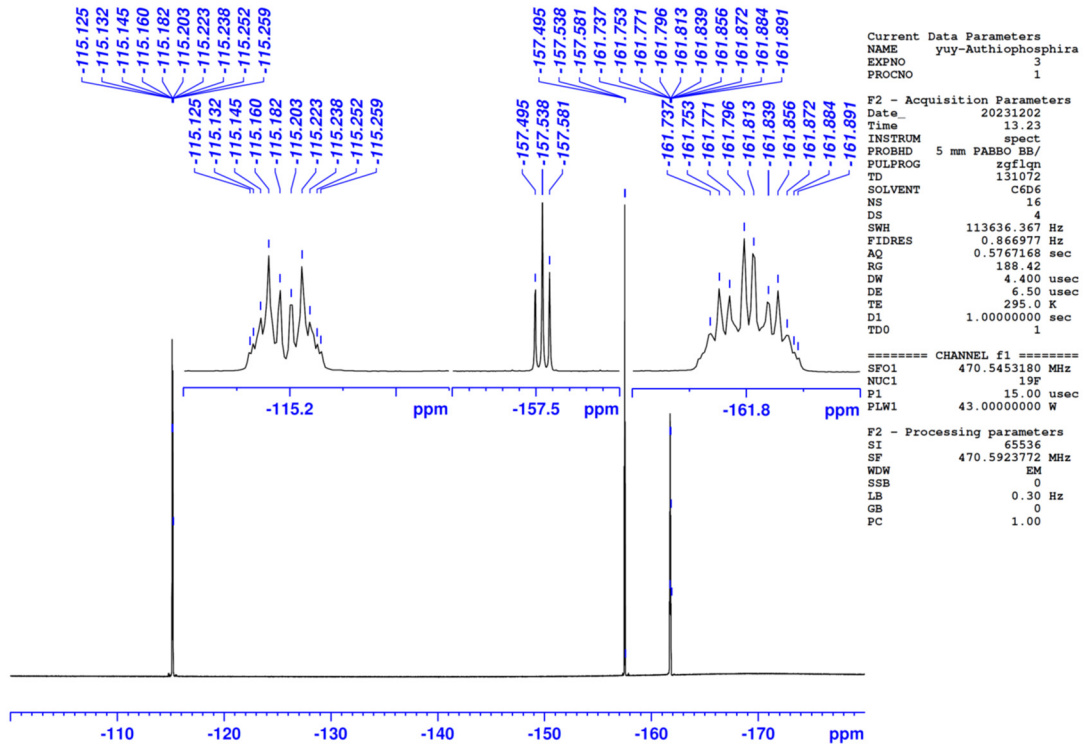

Fig. S37 ^{19}F NMR spectrum of **5Au** in C_6D_6 at 295 K.

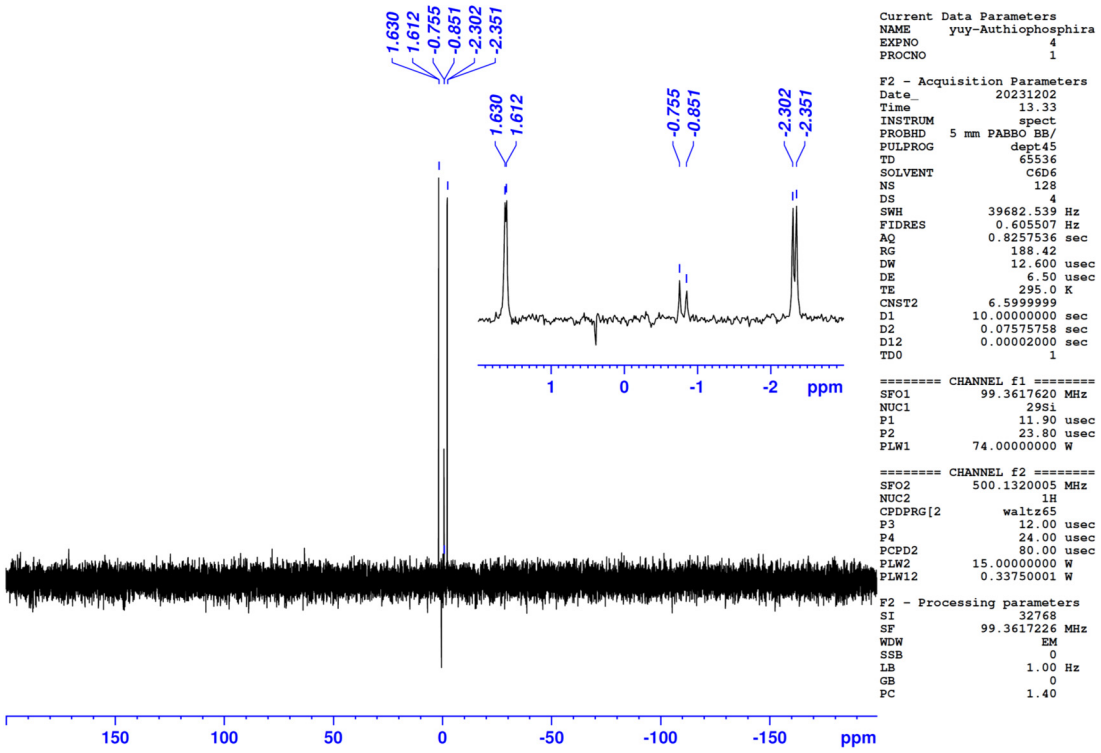

Fig. S38 $^{29}Si\{^{1}H\}$ (dept45) NMR spectrum of **5Au** in C_6D_6 at 295 K.

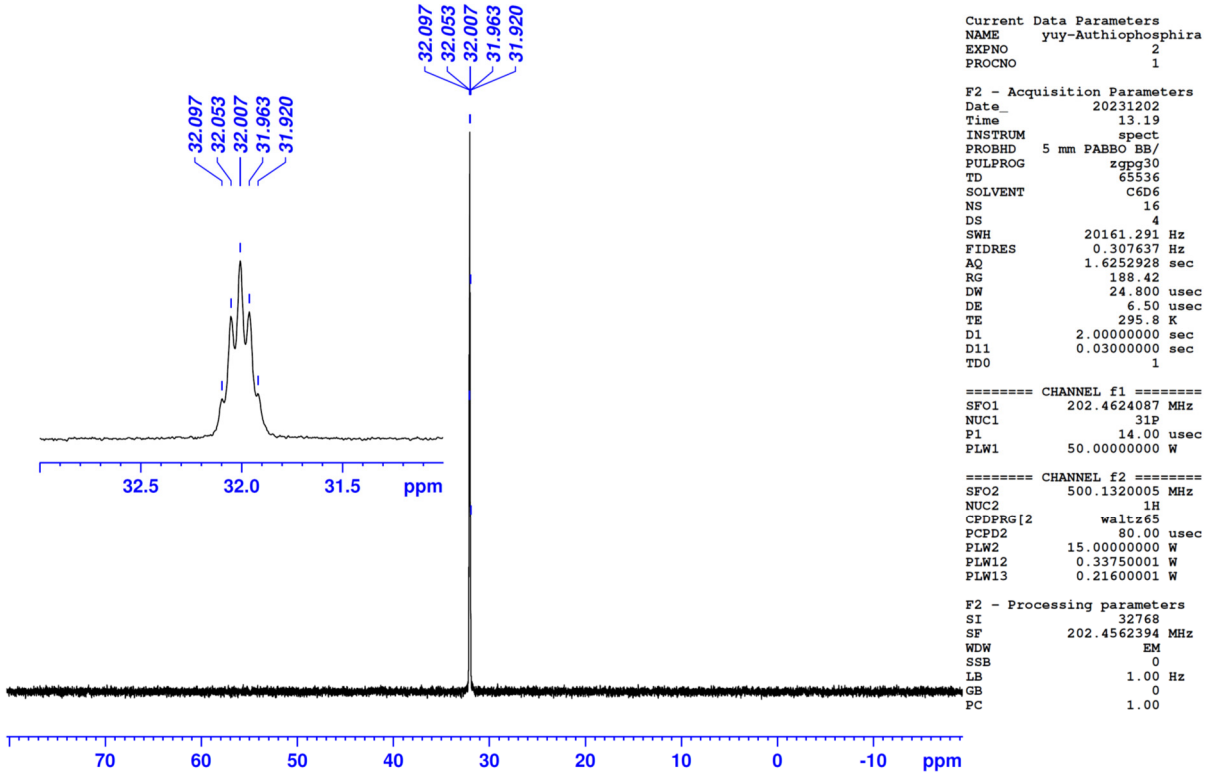

Fig. S39 $^{31}P\{^{1}H\}$ NMR spectrum of **5Au** in C_6D_6 at 296 K.

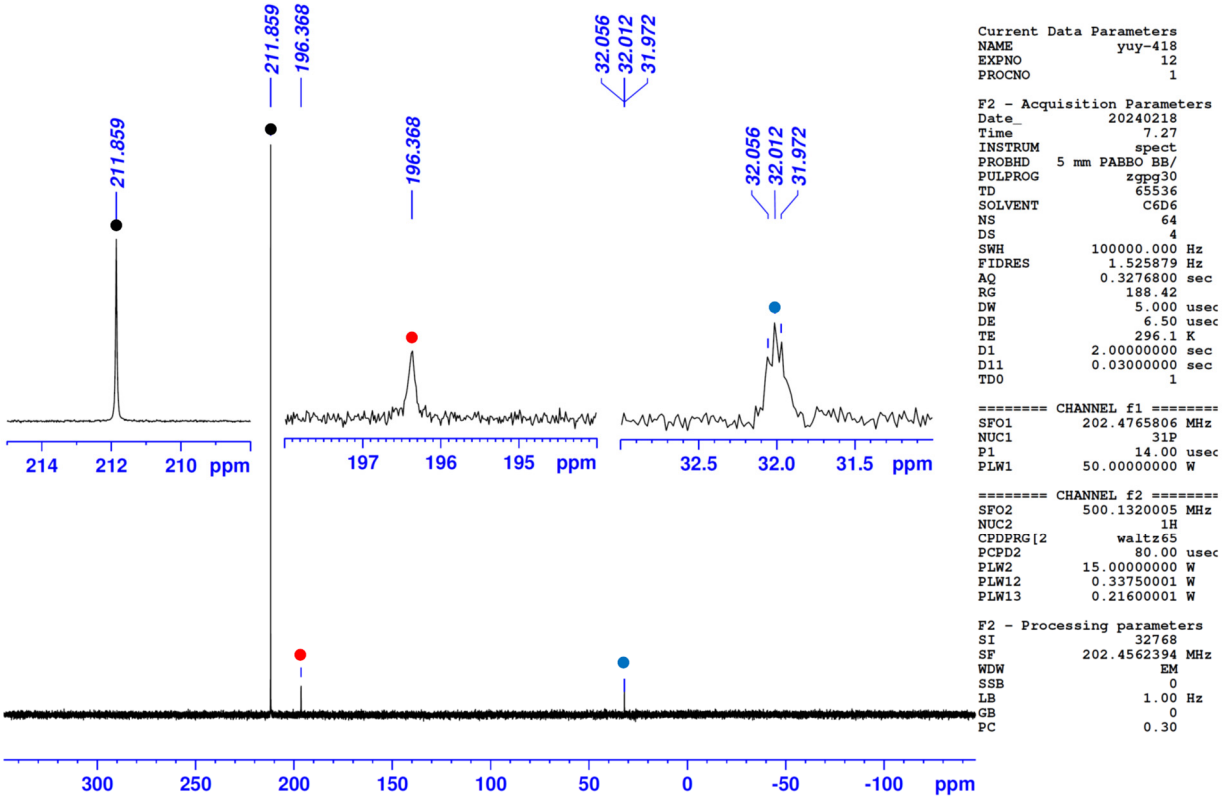

Fig. S40 $^{31}P\{^{1}H\}$ NMR spectrum of the reaction mixture of **3** and $Au(C_6F_5)(tht)$ in C_6D_6 at 296 K (• = **3**, • = **3Au**, • = **5Au**).

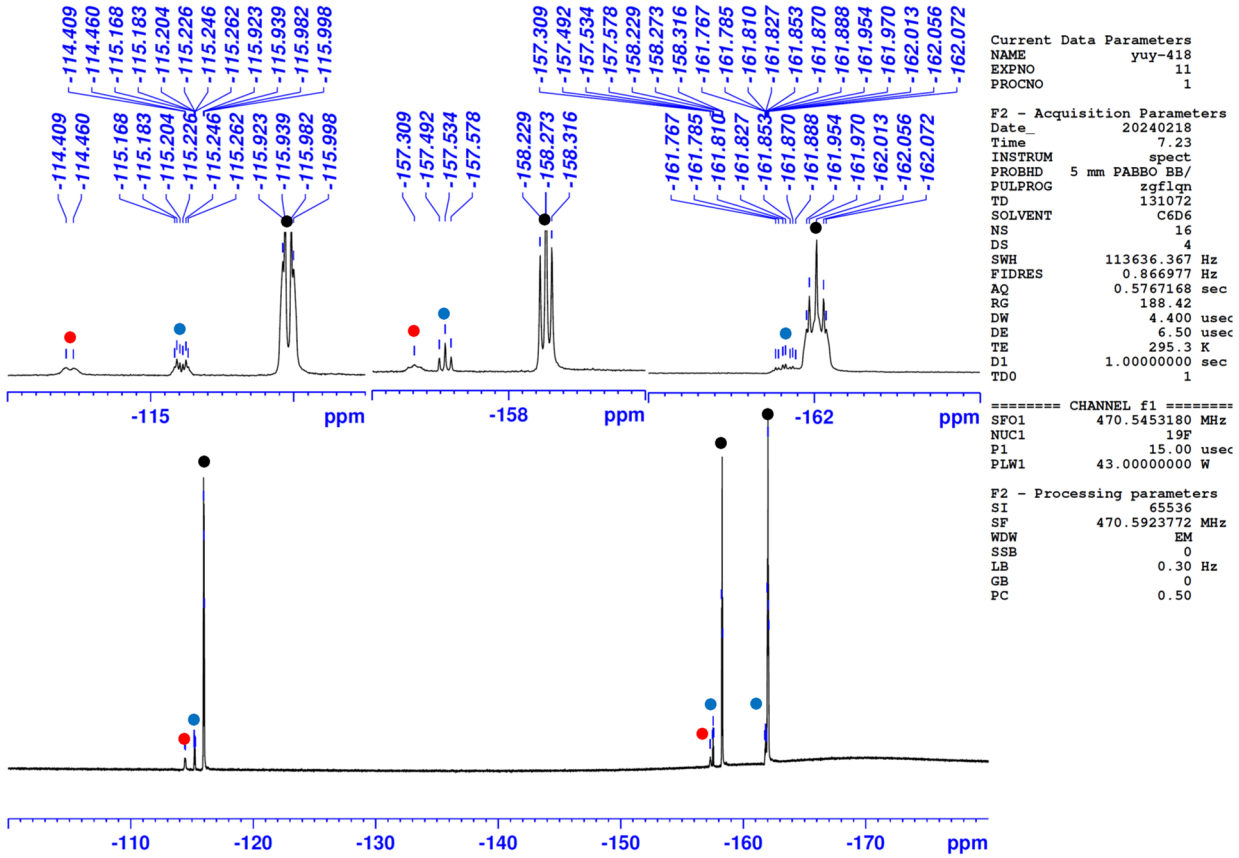

Fig. S41 $^{19}F\{^{1}H\}$ NMR spectrum of the reaction mixture of **3** and $Au(C_6F_5)(tht)$ in C_6D_6 at 295 K (• = $Au(C_6F_5)(tht)$, • = **3Au**, • = **5Au**).

3. Single Crystal X-ray Diffraction Analysis

Single crystals suitable for X-ray diffraction study were obtained by recrystallization under the following conditions: from hexane at room temperature for **1**, **5**, **5Au**, **6** and (2) from hexane at −30 °C for **3**. Single crystal for data collection was coated with paratone oil and mounted on a glass fiber, and then transferred to the cold gas steam of the diffractometer. X-Ray diffraction data were collected on a Rigaku XtaLAB AFC10 diffractometer or Synergy-DW diffractometer with HyPix-6000 hybrid pixel array detector using a graphite monochromated Mo-Kα radiation (λ= 0.71073 Å). Data reduction, scaling, and absorption corrections were performed using CrysAlisPro 1.171.40.39a (Rigaku Oxford Diffraction, 2019) for AFC10 or CrysAlisPro 1.171.42.98a (Rigaku Oxford Diffraction, 2023) for Synergy-DW. Empirical absorption corrections based on the multiple measurement of equivalent reflections were applied using spherical harmonics implemented in SCALE3 ABSPACK scaling algorithm. The structures were solved by direct method and refined by full-matrix least squares against F^2 using all data (SHELXL-2019)[S3]. Molecular structures were analyzed by Yadokari-XG software.[S4]

Crystal Data of **1** (CCDC-2345108) (90 K)

$C_{36}H_{48}ClPSi_4$; FW 659.52; Monoclinic; space group $P2_1/n$, a = 16.1335(5) Å, b = 13.1016(3) Å, c = 16.7859(4) Å, β = 91.240(2)° V = 3547.28(16) Å^3, Z = 4, $R1$ = 0.0513 ($I>2\sigma(I)$), $wR2$ = 0.1255 (all data), GOF = 1.113.

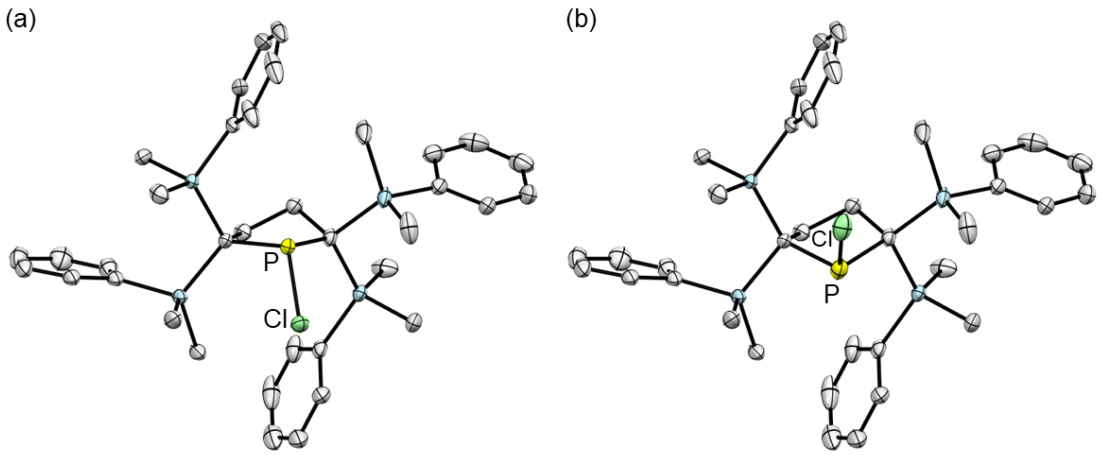

Fig, S42 ORTEPs of **1**. Thermal ellipsoids are shown at 50% probability level. The P–Cl moiety is disordered with a ratio of 80:20. (a) major part and (b) minor part.

Crystal Data of **3** (CCDC-2345109) (100 K)

$C_{28}H_{37}PSSi_3$; FW 520.87; Monoclinic; space group $P2_1/c$, a = 13.2702(3) Å, b = 12.9600(2) Å, c = 17.3599(3) Å, β = 107.126(2)°, V = 2853.20(10) Å^3, Z = 4, $R1$ = 0.0296 (I>2σ(I)), $wR2$ = 0.0818 (all data), GOF = 1.035.

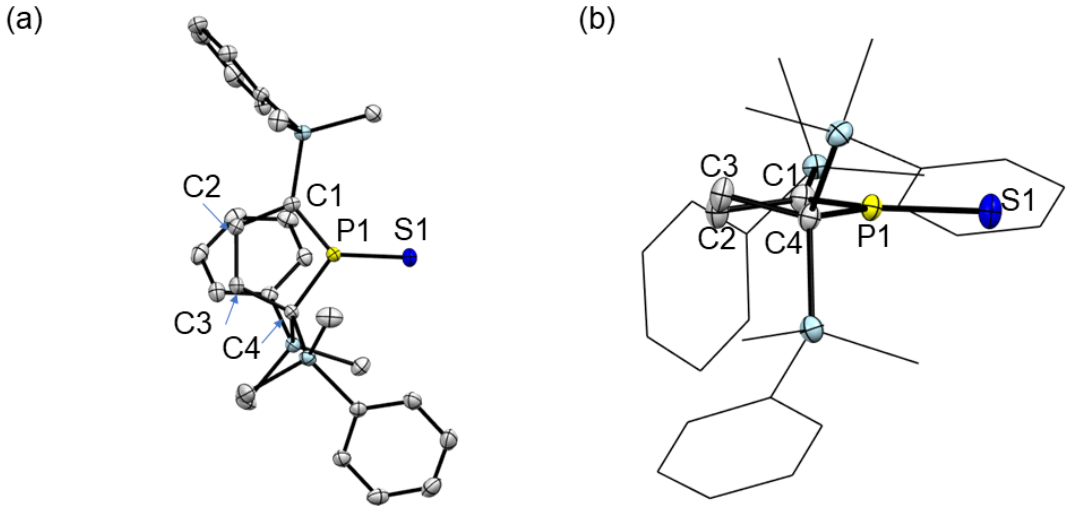

Fig. S43 ORTEPs of **3**. Hydrogen atoms was omitted for clarity. Thermal ellipsoids are shown at 50% probability level. (a) Top View; (b) Side View.

Crystal Data of **5** (CCDC-2345110) (100 K)

$C_{28}H_{37}PSSi_3$; FW 520.87; Monoclinic; space group $P2_1/c$, a = 13.1508(2) Å, b = 9.7019(1) Å, c = 22.7273(3) Å, α = 90°, β = 101.809(2)°, γ = 90°, V = 2838.35(7) Å^3, Z = 4, $R1$ = 0.0261 (I>2σ(I)), $wR2$ = 0.0706 (all data), GOF = 1.026.

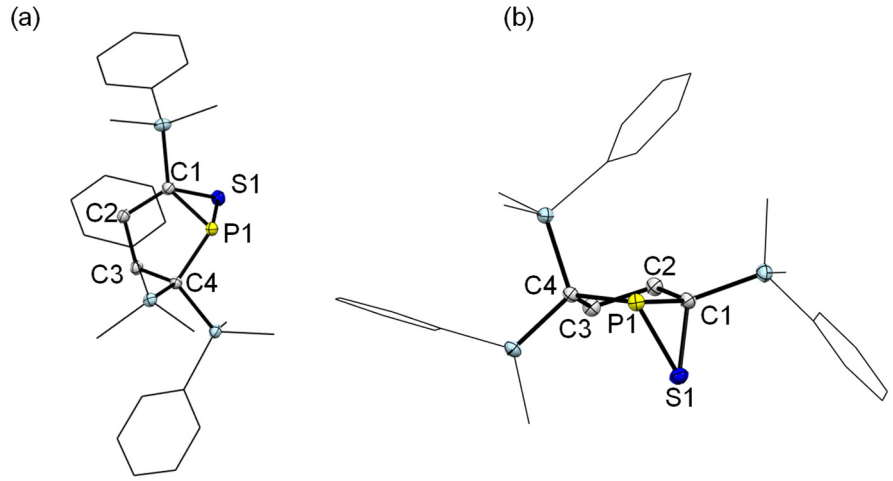

Fig. S44 ORTEP of **5**. Hydrogen atoms was omitted for clarity. Thermal ellipsoids are shown at 50% probability level. (a) Top View; (b) Side View.

Crystal Data of **6** (CCDC-2345107) (150 K)

$C_{28}H_{37}PS_2Si_3$; FW 552.93; Monoclinic; space group $P2_1/n$, a = 17.3438(4) Å, b = 7.4997(2) Å, c = 23.1443(6) Å, β = 91.611(2)°, V = 3009.27(13) Å^3, Z = 4, $R1$ = 0.0468 (I>2σ(I)), $wR2$ = 0.1178 (all data), GOF = 1.086.

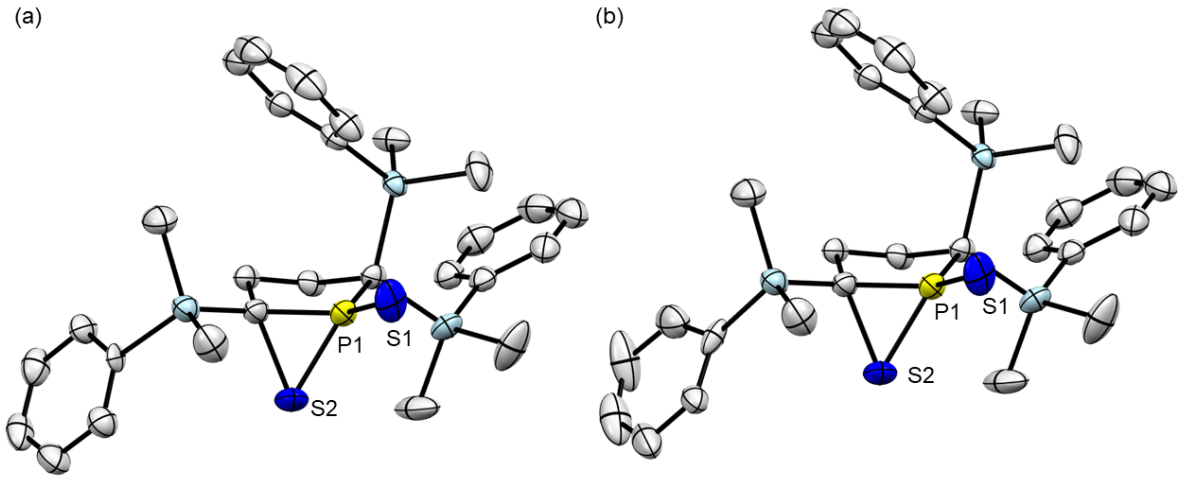

Fig. S45 ORTEP of **6**. Hydrogen atoms were omitted for clarity. Thermal ellipsoids are shown at 50% probability level. One of four phenyl groups in the bottom left is disordered with a ratio of 63:37. (a) major part and (b) minor part.

Crystal Data of **5Au** (CCDC-2345111) (100 K)

$C_{36}H_{37}AuF_5PSSi_3$; FW 884.90; Triclinic; space group *P*-1, a = 13.87560(10) Å, b = 20.18150(10) Å, c = 25.9410(2) Å, α = 88.5250(10)°, β = 91.611(2)°, γ = 75.6800(10)°, V = 7032.08(9) Å^3, Z = 8, $R1$ = 0.0293 ($I>2\sigma(I)$), $wR2$ = 0.0576 (all data), GOF = 1.019.

(a)

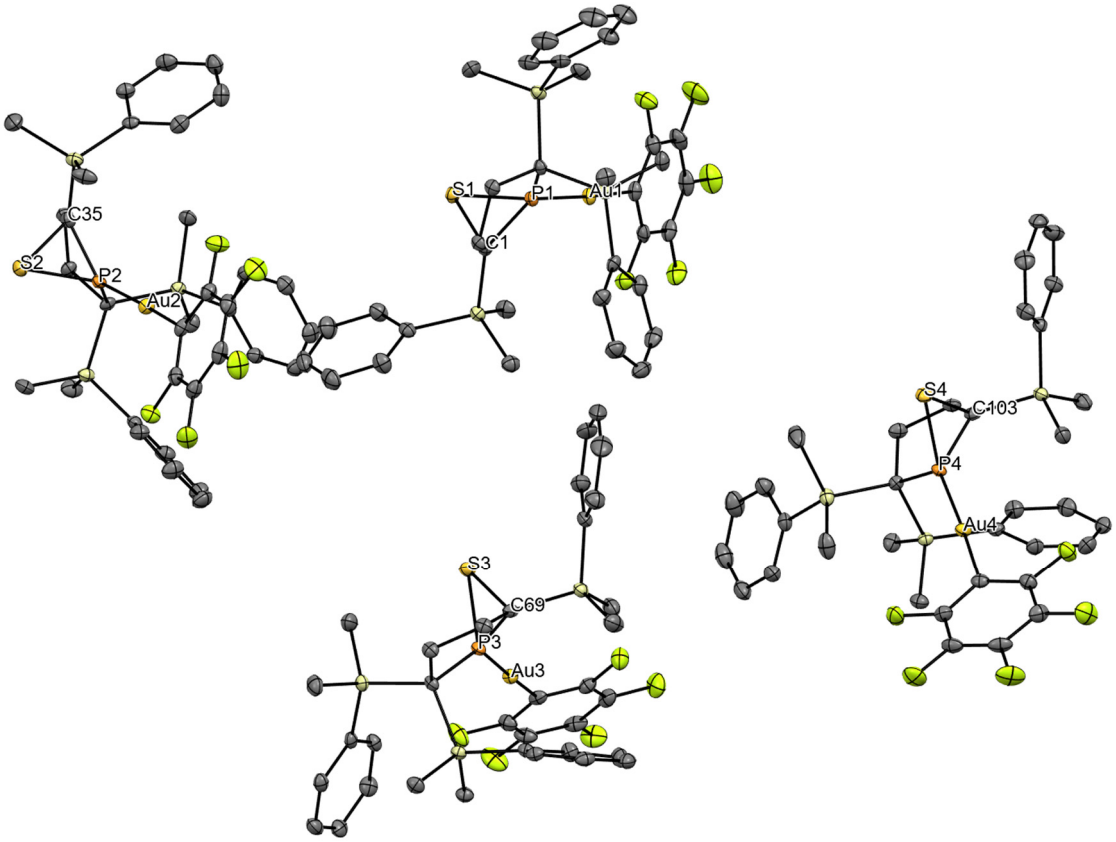

(b)

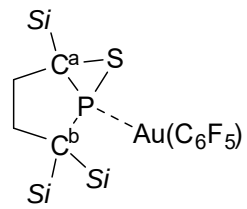

5Au (*Si* = $SiMe_2Ph$)

Fig. S46 (a) ORTEP of **5Au**. Hydrogen atoms was omitted for clarity. Thermal ellipsoids are shown at 50% probability level. Crystallographically four independent molecules exist in the asymmetric unit. These molecules have almost the same structure. **5Au** has an almost linear two coordinate gold(I) complex [angle P1–Au–C_6F_5: 173.91(8)°], and the phosphorus atom coordinates to the gold atom. Intra- or intermolecular Au-S and Au-Au contacts are not found. (b) Averaged bond lengths (Å) and angles (°) around the thiaphosphirane moiety: P–Au 2.2607(7), P–C^a 1.808(3), P–C^b 1.818(3), P–S 2.0848(10), C^a–P–C^b 99.32(13), C^a–P–S 57.22(9), C^b–P–S 108.44(10). P–C^a–S 69.95(4), C^a–S–P 54.67(3).

4. Theoretical Calculations

All theoretical calculations were performed using Gaussian 09,[S5] GRRM 14,[S6] NBO7.0[S7] (for NBO analysis, Wiberg bond index, and NRT analysis), and Multiwfn programs (MBO analysis),[S8,S9] IBOview (IBO analysis).[S10,S11] Geometry optimization and frequency analysis were carried out at the B3PW91-D3/B1 level of theory (B1: SDD for Au and Cu, 6-31G(d) for other atoms) unless otherwise noted. Atomic coordinates of the optimized structures were summarized in the "structures.xyz" file. No imaginary frequencies were found in the equilibrium structures of all compounds and one imaginary frequency was found in the transition states. Reaction mechanisms were investigated by using a combination of SADDLE job types in the GRRM program and each TS was checked by IRC analysis. Intrinsic Bond Orbitals (IBOs) were calculated and visualized with IboView (Version 20211019) starting with the wavefunction constructed PBE/def2-SVP basis set.

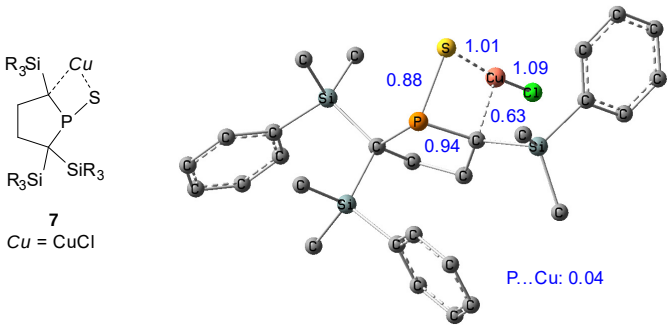

Fig. S47 Selected Mayer bond order of **7**.

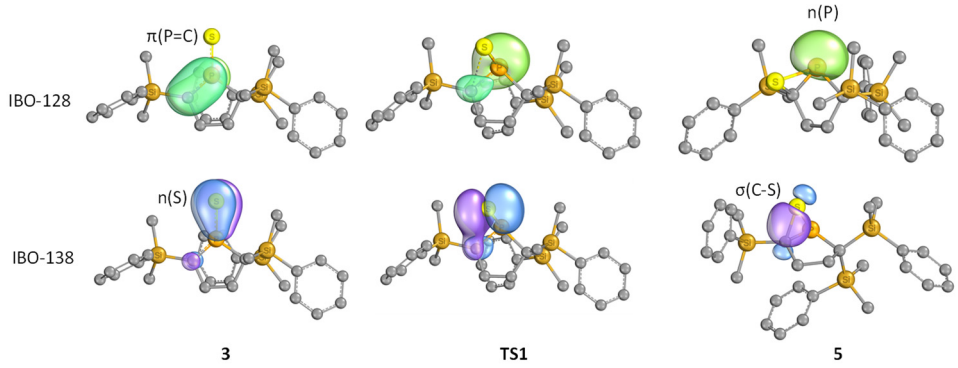

Fig. S48 Selected intrinsic bond orbitals (IBOs) of **3**, **TS1**, and **5**.

Table. S1 Experimentally Obtained and Calculated ^{31}P NMR Chemical Shifts of **1-6**, **5Au**, and **3Au**

	Compounds								
Chemical Shift δ(^{31}P)	**1**	**2**	**3**	**4**	**5**	**6**	**5Au**	η^2-P,S-**3Au**	η^2-P,C-**3Au**
Experimental (C_6D_6)	+199.4	+138.1	+211.9	+327.8	–29.6	+42.0	+32.0	+196.4	
Calculated*	**+243.7**	**+201.0**	**+225.8**	**+362.0**	**+0.5**	**+64.2**	**+12.0**	**+144.9**	**+220.6**

*GIAO-revTPSS/def2-TZVP (PCM: benzene) level

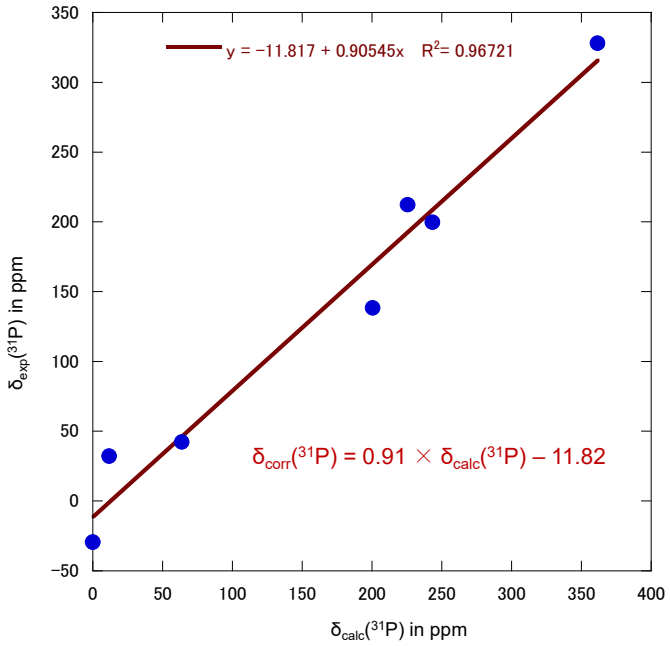

Fig. S49 (a) Linear relationship between experimentally obtained ^{31}P NMR chemicals shifts [$\delta_{exp}(^{31}P)$] and GIAO-calculated chemical shifts [$\delta_{calc}(^{31}P)$]. According to the relationship, corrected chemical shifts [$\delta_{corr}(^{31}P)$] were given by the following equation: $\delta_{corr}(^{31}P) = 0.91 \times \delta_{calc}(^{31}P) - 11.8$.

5. References

S1 I. Fleming and U. Ghosh, *J. Chem. Soc., Perkin Trans. 1,* 1994, 257–262.

S2. T. Lauterbach, M. Livendahl, A. Rosellón, P. Espinet and A. M. Echavarren, *Org. Lett*., 2010, **12**, 3006–3009.

S3. G. M. Sheldrick, *Acta Cryst.* 2015, **C71**, 3–8.

S4. Yadokari-XG 2009, Release of Software for Crystal Structure Analyses, C. Kabuto, S. Akine, T. Nemoto and E. Kwon, *J. Cryst. Soc. Jpn.* 2009, **51**, 218–224.

S5. Gaussian 09, Revision D.01, M. J. Frisch, G. W. Trucks, H. B. Schlegel, G. E. Scuseria, M. A. Robb, J. R. Cheeseman, G. Scalmani, V. Barone, B. Mennucci, G. A. Petersson, H. Nakatsuji, M. Caricato, X. Li, H. P. Hratchian, A. F. Izmaylov, J. Bloino, G. Zheng, J. L. Sonnenberg, M. Hada, M. Ehara, K. Toyota, R. Fukuda, J. Hasegawa, M. Ishida, T. Nakajima, Y. Honda, O. Kitao, H. Nakai, T. Vreven, J. A. Montgomery, Jr., J. E. Peralta, F. Ogliaro, M. Bearpark, J. J. Heyd, E. Brothers, K. N. Kudin, V. N. Staroverov, T. Keith, R. Kobayashi, J. Normand, K. Raghavachari, A. Rendell, J. C. Burant, S. S. Iyengar, J. Tomasi, M. Cossi, N. Rega, J. M. Millam, M. Klene, J. E. Knox, J. B. Cross, V. Bakken, C. Adamo, J. Jaramillo, R. Gomperts, R. E. Stratmann, O. Yazyev, A. J. Austin, R. Cammi, C. Pomelli, J. W. Ochterski, R. L. Martin, K. Morokuma, V. G. Zakrzewski, G. A. Voth, P. Salvador, J. J. Dannenberg, S. Dapprich, A. D. Daniels, O. Farkas, J. B. Foresman, J. V. Ortiz, J. Cioslowski and D. J. Fox, Gaussian, Inc., Wallingford CT, 2013.

S6. GRRM 14: S. Maeda, Y. Harabuchi, Y. Osada, T. Taketsugu, K. Morokuma and K. Ohno, see http://grrm.chem.tohoku.ac.jp/GRRM/; S. Maeda, K. Ohno and K. Morokuma, *Phys. Chem. Chem. Phys*., 2013, **15**, 3683–3701.

S7. NBO 7.0: E. D. Glendening, J. K. Badenhoop, A. E. Reed, J. E. Carpenter, J. A. Bohmann, C. M. Morales, P. Karafiloglou, C. R. Landis and F. Weinhold, Theoretical Chemistry Institute, University of Wisconsin, Madison (2018).

S8. Multiwfn: T. Lu and F. Chen, *J. Comput. Chem*., 2012, **33**, 580-592.

S9. I. Mayer, *J. Comput. Chem*., 2016, **28**, 204-221.

S10. (a) G. Knizia, *J. Chem. Theory Comput*., 2013, **9**, 4834–4843; (b) G. Knizia and J. E. M. N. Klein, *Angew. Chem., Int. Ed*., 2015, **54**, 5518–5522.

S11. IBO View: G. Knizia, see http://www.iboview.org.